B. Sc. Thesis

Upgrade of the Graphitization System for ^{14}C AMS Analyses

Division of Nuclear Physics

Lund University

LUND
UNIVERSITY

By: Philip Dalsbecker

Supervisor: Prof. Kristina Eriksson Stenström

June 5th, 2013

Abstract

For decades, accelerator mass spectrometry (AMS) has been used for radiocarbon dating. The background of this technique is outlined along with an in-depth look at the graphitization process used to prepare samples for AMS analysis. The technology necessary to achieve the vacuum quality needed in graphitization and accelerator mass spectrometry is discussed as well.

The graphitization system belonging to the division of nuclear physics at Lund University is modernized and tested, and four different kinds of standard samples are graphitized and analysed using the Lund Single-Stage Accelerator Mass Spectrometer. The results deviate to some extent from the expected values, and the most likely reason is that the cracker used to crack open sealed quartz tubes is faulty. Leaks of air into the system would explain the deviations, and while the rest of the graphitization system has undergone extensive leak detection, no tests have been performed to determine whether the cracker lets air into the system upon cracking a tube or begins to do so as a result of the cracking. The upgrade is deemed successful, however, as the reactors replacing the former ones have passed the extensive leak detection and the pressure transducers have proven themselves to function as expected.

A calculation of the maximal conductance and throughput of the Fysicum graphitization system are performed as well, with the former being found to be $1.45 \cdot 10^{-3}$ m^3/s and the latter being approximately 169W.

Acknowledgements

I wish to thank my supervisor, Prof. Kristina Eriksson Stenström, for helping and guiding me through the process of modernizing the Fysicum graphitization system and for helping me to better understand the world of experimental physics.

I would also like to thank research engineerMattias Olsson for his help and valuable advice regarding the process of graphitization and the redesigning of the Fysicum graphitization setup.

Futhermore, I would like to thank Dr. Mikael Elfman for his advice regarding the electronics involved in the data acquisition, and research engineer Mikael Ekholm for helping me with several practical steps in the redesign of the graphitization setup.

Last but absolutely not least, I wish to thank my family for always helping, supporting and believing in me.

Table of contents

Introduction

Carbon is one of the most abundant elements in the Universe, and is part of all life-forms we know of. It exists in three naturally occurring isotopes, all with the same number of protons (six) but with different numbers of neutrons. The isotopes with six and seven neutrons are stable, whereas the isotope with eight neutrons, called carbon-14 or ^{14}C, is radioactive with a half-life of approximately 5730 years. The atmospheric amount of this carbon isotope is replenished in the atmosphere through interactions with cosmic rays, and so remains to a first approximation constant in the atmosphere. Plants absorb carbon dioxide through photosynthesis, and animals then feed on these plants or one another. Thus, the carbon isotope ratios in the atmosphere are reflected in all higher life-forms for as long as they eat and breathe, but as they die, this ratio will begin to shift in favour of the stable isotopes as the radioactive isotope beta-decays into nitrogen. For this reason, carbon-14 has a history of being used for dating purposes. Knowing what the atmospheric carbon ratios were in the past, it is possible to perform very accurate dating by comparing the ratios in a sample today; the question becomes simply how to count the number of atoms of each isotope in a sample.

The method discussed in this thesis is called accelerator mass spectrometry (AMS), which is a very precise method of doing just that: counting atoms. Using AMS, a sample 10000 years old can be dated to within ±40 years in less than an hour [Hellborg and Skog, 2008]; it is estimated that radiocarbon dating with AMS is possible with samples up to 50'000 years of age, if the sample used is well enough preserved.

An important step in the process of AMS dating is the conversion of a carbonaceous sample into elemental carbon, which can be used in the accelerator. This process, called graphitization, is the main focus of this thesis work. The carbonaceous sample is combusted and oxidised into carbon dioxide, which is subsequently reduced into solid, elemental carbon for AMS analysis. The main aim of this thesis work is to modernize and test the existing graphitization setup at Lund University's Division of Nuclear Physics, as well as provide a detailed overview of the processes of graphitization and accelerator mass spectrometry. Furthermore, the basics of vacuum science and technology are elaborated upon, as vacuum techniques are vital to both graphitization and AMS, and the physical background of radiocarbon dating is briefly discussed. The purpose of this thesis is to grant both theoretical and practical insight into the many aspects of accelerator mass spectrometry as a tool for radiocarbon dating, portraying not only the underlying physical processes but also the extensive practical and experimental work that makes the dating techniques possible. As the main practical work involves a modernization and testing of the graphitization setup, much emphasis will be placed on this and the testing procedure will be discussed in detail, enabling future use of parts of this thesis as an instruction of the operation of the Fysicum graphitization system.

However, this thesis will not evaluate the methods involved in graphitization, nor go beyond merely describing the main methods of accelerator mass spectrometry. The modernization performed in this upgrade of the Fysicum system involves the ovens, reactor volumes and pressure measurement technology, but will not attempt to evaluate the way in which the graphitization is performed, nor go beyond a brief comparison of single-stage and tandem AMS in terms of evaluating AMS techniques. The basics of radiocarbon dating will be discussed, but no calculations will be performed, nor will the calculation methods be discussed.

Accelerator mass spectrometry

In this section, the basic principles of tandem AMS will be described, whereupon the differences between this and single-stage AMS (SSAMS, the type which is employed at Geocentrum in Lund) will be outlined.

Background

The use of accelerators in mass spectrometry dates back as far as 1939, when two physicists at Berkeley, Alvarez and Cornog, made use of a cyclotron to separate ^{3}He from ordinary helium [Alvarez &Cornog, 1939; Kutschera, 1986]. However, despite the successful use of the cyclotron, the field of accelerator-based mass spectrometry saw hardly any development for several decades. Not until the 1970's did the next wave of development begin in accelerator mass spectrometry, with the introduction of Van de Graaff electrostatic tandem accelerators into the field of AMS, and as they surged in popularity, cyclotron-based AMS became increasingly popular as well [Krane, 1988]. Scientists began to realize that mass spectrometry using these methods had several benefits, such as a very high precision which enabled the counting of atoms, leading up to a revolution in dating with long-lived radioisotopes [Kutschera, 1986]. The use of tandem accelerators grew very quickly, partly due to the fact that many laboratories had access to such accelerators that were no longer in use, as described by Hellborg and Skog[2008]. The core principle of accelerator mass spectrometry is to count different isotopes of elements and compare their ratios to the established standards of isotope abundance. It was first done for helium, as mentioned above, but has also been done with aluminium, chlorine, beryllium, iodine, carbon and several other elements, according to Litherland [1984].

Ionization

The first step in all AMS systems is the ion source. Here, in the typical case, negative ions are to be formed, which are then to form a stable and efficient beam leading into the rest of the system. In the case of a solid sample, the sputtering ion source commonly works as follows, as described by Hellborg and Skog [2008]:

Cesium vapour is released by heatingmetallic cesium in an oven and led to a heated ionizing plate of tantalum where it is ionized. Being an alkali metal, it forms Cs^{+} ions, so it is important to make sure that the sample, which is kept in the same volume, has a negative potential for the gas ions to be attracted to. This speeds up the ions, which upon impact with the surface will knock out atoms and ions from the sample. Since the sample has negative potential, positive ions will be drawn back towards the sample, neutral atoms will scatter having felt no noticeable Coulomb force, and negative ions will be repelled by the sample, giving rise to the beam. As it is led out through an opening in the ion source, the beam is further accelerated by a potential difference in a short voltage gap before entering the injector. There is a special benefit associated with the use of a negative-ion source in the measurement of some radioisotopes such as ^{14}C, in that there are isobars (in that case, ^{14}N) which cannot form stable negative ions and will thus be removed from the background.However, there will still be certain molecular isobars which form negative ions and survive the sputtering, such as (in the case of ^{14}C) $^{13}CH^{-}$ and $^{12}CH_2^{-}$. Since the stable carbon isotopes are much more abundant than ^{14}C, with the rare isotope representing only about 10^{-10}% of the carbon in a modern sample, there is need for analysis and selection before the ions reach the detectors, lest the much more abundant molecular isobars will alter the isotope ratios.

Injection

The injector itself contains one or several analysing magnets and often some electrostatic analysing component as well, along with quadrupole lenses to focus the beam. The injector can be of two

different types, sequential or simultaneous. The former switches the attractive voltage on the casing of the analysing magnets to allow for different ions to pass by changing their momenta and kinetic energies, allowing either the rare ion to be counted or the stable ion required for normalization to pass. Therefore, the different ions are not injected at the same time but rather sequentially. Most of the time is spent on the rare isotope, as discussed by Fifield [1999], since it takes shorter time intervals to obtain plenty of stable ions. The switching between the isotopes is very fast, the pulses of stable isotopes being merely 100 µs long. The reason for the fast switching is that the isotopes can be treated as being detected simultaneously; if there are fluctuations in the system, all isotopes will be affected similarly. Simultaneous injection, on the other hand, injects them together, using magnets to separate the isotopes into different trajectories, keeping them apart for their duration in the injector, before being magnetically recombined in the final step, as described by Hellborg and Skog [2008]. The injector then injects the selected beam components into the accelerator.

Stripping and acceleration

The tandem accelerator is equipped with a high-voltage terminal, providing voltages of the order of megavolt, towards which the ions are accelerated. Before entering the accelerating part, however, the beam is first focused with an Einzel lens, as can be seen in Fig. 1. This kind of beam focusing lens consists of a beam pipe which is split up into several parts with different voltages applied. For a three-part setup, the first and third segments are at ground potential whereas the second has a positive voltage. The beam first diverges, then converges upon a focal point, whereupon it diverges again.

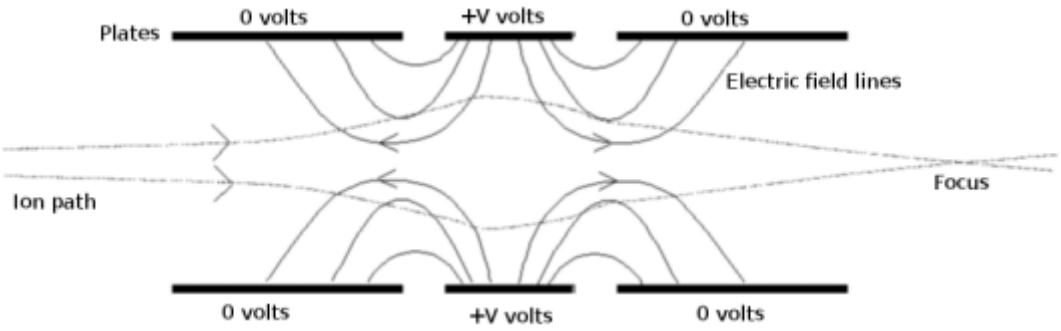

Figure 1: focusing of a negatively charged beam by means of an Einzel lens. Figure obtained from http://commons.wikimedia.org/wiki/File:Einzel_lens.png as of 2013-05-24. Creator: Wikiezz.

The tube leading to the accelerating component is fitted with several electrode plates perpendicular to the beam direction, each having a circular aperture in the center. These form what is called an electrostatic aperture lens. The field strength increases for each electrode the beam passes through, providing a continuous strong focusing of the formerly divergent beam. Having been focused, the ions are subsequently accelerated towards the high-voltage terminal. Next, the ions pass through either a specific gas compartment or a thin foil [Hellborg& Skog, 2008]. Upon passing, the atoms are stripped of enough many electrons that the ions change their charge from negative to positive, meaning that they can be further accelerated towards a much lower potential, typically ground. In the stripping process, the energy with which the ions enter the stripping chamber is of importance, as discussed by Wiebert et al [1995]; the greater the energy, the greater will the average charge state be when the ions have been stripped. The most common stripping method is the gas-based one, often with a mechanism that pumps back gas that seeps out of the compartment, rather than letting it out into the accelerator system [Hellborg& Skog, 2008]. In order to avoid the beam creating sparks and losing intensity, air is rarely used for high-voltage systems; typically sulphur hexafluoride or some other gas with high dielectric strength is used. A special benefit of the stripping system is that the

process has a good chance of dissociating molecular isobars, since it may put them in charge states which are unstable, leading to a molecular dissociation, the fragments of which will be removed in the next step of the analyser.

Analysis and detection

Shortly after passing the second acceleration stage, the beam is typically focused again, e.g. by means of a magnetic lens, before entering another magnetic analyser. The main purpose of this is to rid the beam of the molecular fragments which were broken up in the stripping process. The sequence of lenses and analysers varies between single-stage and tandem AMS as well as between AMS systems of the same type. The purpose of the analysers is that the rare ions can carry on through the setup, whereas the more abundant ions can be caught at specific points in the analyser if necessary. These ion currents can then be measured by Faraday cups. These cups capture the calibration ions and measure their current, as described by Case Technology Inc. [1999]. The cups are shielded by a magnetic field, preventing electrons from entering. When a positive ion is caught by the cup, the charge is compensated by the ion absorbing as many electrons as it needs to become neutral again. When this happens many times, there will be a general imbalance of charges, since there are too few electrons in the capture area. Electrons will then come from the other terminal of the Faraday cup setup, which is connected to ground. These electrons will pass a current meter, which will show the amount of electrons that are transferred to the cup and thus, knowing the average charge state of the incident ions, the amount of ions can be known. In ^{14}C AMS, these are used to measure the contents of ^{12}C and ^{13}C, which are far more abundant than ^{14}C; the Faraday cups are precision enough for such proportions. The remaining beam, which has not been led to Faraday cups, is generally focused further and made to pass through further analysing components before finally reaching the detector. These detectors come in several different types, some of which are, according to Hellborgand Skog [2008]:

- Gas ionization detectors, in which the beam enters a gas compartment, where the beam particles are slowed down by interactions with the gas. Electrons are knocked off, which are led by means of an electric field to a series of anodes. Each anode collects those electrons that are closest to it, and by keeping track of these signals, one can map how the ions lose energy along their trajectories. Since the energy loss per length unit travelled through the gas varies depending on the nuclear charge, one can also separate isobars with the same total energy.
- Surface barrier detectors, basically a solid-state semiconductor-based equivalent of the gas ionization device. However, they lack the ability of tracking the ions as they gradually lose energy, showing only the total energy of the incoming ion. If all expected remaining isotopes and isobars differ significantly in energy, this kind of detector may be sufficient, otherwise these are typically coupled with gas ionization detectors, catching the ions after they have lost energy to the gas.
- Time-of-flight detectors, mainly a resolution additive to the systems above, utilized when dealing with heavy ions for which distinction between near-isobars is difficult. The detector begins with a start-signal device, generally a carbon foil, which takes up very little of the energy of the heavy ions. The passage causes electrons to be emitted from the foil, which are subsequently picked up by a detection system in order to get a primary signal, indicating entry into the detector. A few meters further along the beam path is typically either another foil producing a similar signal, followed by a detector system as described above, or simply a silicon surface barrier detector doubling as stop-signal generator. The TOF system gives the

time between the signals, and the detector system gives the total energy. Together, they can discern between heavy isotopes such as iodine-127 and -129.

- Two other well-known methods are gas-filled magnets, in which the stripping of electrons takes place in the magnetic detection device, and particle-induced X-ray emission, which involves emission of X-rays depending on the ions passing through and the atoms in the detector material. However, neither of these is employed in carbon AMS, and therefore they will not be dealt with here.

Single-stage AMS

Developed for National Electrostatics Corporation in 2002 [Patent Lens, 2013], the single-stage AMS (or SSAMS) is a variation of AMS which operates at very low voltage (less than 300 kV) offering slightly less precision than the tandem systems [Klody et al., 2005]. The sulphur hexafluoride tank design is not used in SSAMS machines, having been replaced by an air volume due to the dielectric strength requirement being markedly lower. There is also, as the name implies, no secondary acceleration stage. The analysers and detectors are located directly after the stripping section, where the second acceleration stage would normally be. The problem that a tandem accelerator faces at this point is that fragments of molecules which were dissociated in the stripper might change charge and energy, having a chance of proceeding along with the ions through to the detector systems. The SSAMS avoids this problem, since while the fragments may change charge, they will not change energy, on account of there not being a second acceleration stage. Thus, the analysing components directly after the stripper will be able to remove the fragments, reducing the background. The advantage of the tandem accelerator comes into play for heavier ions, where the tandem offers significantly higher energies for the ions than the single-stage model [Eriksson Stenström, 2013].

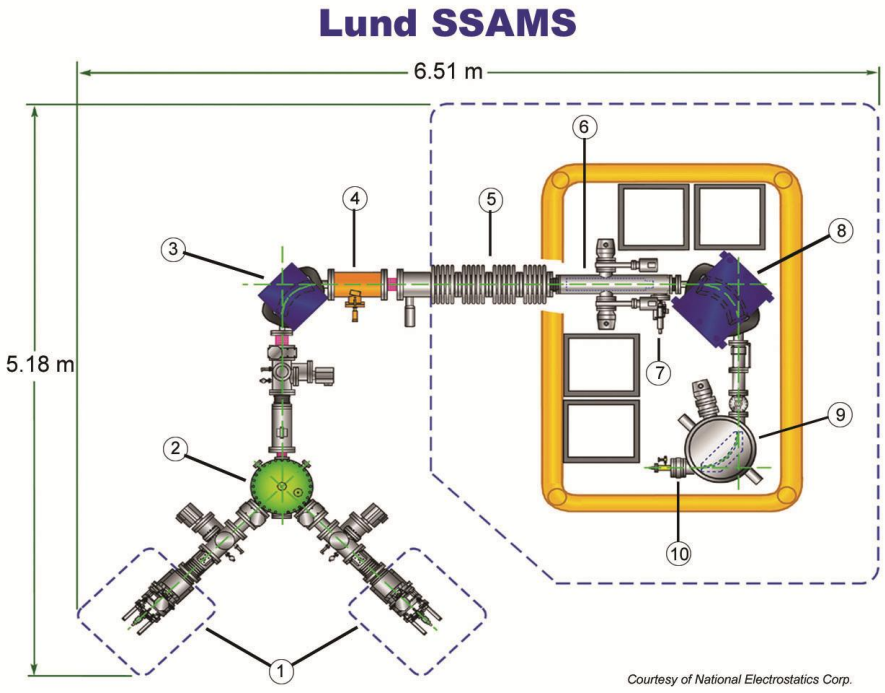

Figure 2: The design of the Lund Single-Stage AMS. 1: ion sources, 2: low-energy electrostatic spherical analyser, 3: low-energy bending magnet, 4: Einzel lens (as seen in Fig. 1), 5: accelerator tube, 6: argon gas stripper, 7: argon valve, 8: high-energy bending magnet, 9: high-energy electrostatic spherical analyser, 10: sequential post-accelerator deflector. Courtesy of National Electrostatics Corp.

The more recent model of the SSAMS, developed for commercial use, has a slightly different structure than what is described above (see Fig. 2) [Klody et al., 2005]. The ion source and injector have ground potential, being accelerated towards the rest of the system, where the potential is at 250 kV. The single-stage model also uses sequential injection, as outlined above. Measurements made with this kind of system were found to have higher precision than what was first expected, and proved itself to be cheaper and more space-efficient, but as the energy is decreased, the risk of losing precision increases.

Analysis

The analysing gear relies purely on electromagnetic principles, which is why it is so important to work with ions. Only they can be accelerated directly by electromagnetic methods, and only they can be manipulated with them. The analysers are mainly of one of the following sorts:

- Electrostatic Spherical Analyser, or ESA, is basically a spherical condenser, capable of both selection and a certain degree of focusing [Purcell, 1938]. Two of these can be seen in Fig. 2, one in the lower-energy part and another one further along the beam line where the ions have higher energies. The selecting part comes from equating a (non-relativistic) particle's centripetal force when in a perfect orbit with the force supplied by the Coulomb law. The equation can be further modified for the (justified) assumption that the electric field and curvature radius of the system are both well known. Then, for a spherical geometry, the equation reads $E \cdot r = \frac{m \cdot v^2}{q}$ or simply $2E \cdot r = \frac{K}{q_{ion}}$ with *E* as electric field, *m* as mass, *v* as speed, *q* as charge and *K* as kinetic energy. Thus, for a given geometry, this setup chooses an energy-to-charge ratio of the particles that pass. With an additional velocity selector, this can be narrowed down to mass-to-charge selection, since velocity is then known.

- Magnetic (bending) analysis is done by means of a magnetic (*B*) field orthogonal to the velocity of the ion beam. As with the ESAs, two of these are seen in Fig. 2, one in the lower-energy part and one after the acceleration stage. By means of the Lorentz force in a space free of electrical fields, the force exerted on each ion is $F = q \cdot v \cdot B$, the force being orthogonal to both *v* and *B*. Thus, the ions will bend in a circular fashion with a bending radius *r*, showing a centripetal force of $F = \frac{m \cdot v^2}{r}$. Equating that expression with the above one, knowing the desired radius and being able to set the B-field as is needed, the equation becomes $B \cdot r = \frac{m \cdot v}{q}$. Thus, the selection is done with respect to the momentum-to-charge ratio, and with an additional velocity selector one can instead work with the mass-to-charge ratio.

- Electromagnetic velocity selector is an important component, since it allows for determination of an exact desired velocity which is allowed to pass while all other velocities are removed. This is done by means of an orthogonal set of E- and B-fields, both perpendicular to the ion beam in such a way that the Lorentz force $\vec{F} = q\left(\vec{E} + \vec{v} \times \vec{B}\right)$ in effect becomes $F = q(E - vB)$. This force is the cause of the deviations from the path of the beam in the selector, and the velocity is chosen as the quotient $v = \frac{E}{B}$. As the detector system is built, a radius of curvature is chosen in each of the previously mentioned analysing systems, if they are both included. It should be said also that several openings out of the magnetic system may be built depending on what ratios are wanted, if several rare isotopes

are of interest. In the electric case, this might be difficult as only one energy gets a circular path, while in the magnet all energies do. Different mass/charge ratios can then be chosen by means of adjusting the fields in the selector and the analyser. However, the two analysers can be used independently of a velocity selector, since the velocity can still be determined as twice the energy *K* divided by the momentum *p*. Having both an electric and a magnetic analyser along with a velocity selector is redundant, however, since both analysers give the mass-to-charge ratio if the velocity is known. In single-stage AMS, this type of selection device is not used at all, since SSAMS machines are equipped with both electrostatic and magnetic analysers.

Vacuum in accelerator science and ^{14}C measurements

In both graphitization, accelerator science and many other experimental applications of physics, good vacuum is essential. In the following section, some of the basic parameters of vacuum are outlined, along with important factors in achieving high-quality vacuum and some of the more common vacuum pumps commercially available today.

The necessity of vacuum

In accelerator systems, the presence of gas molecules can cause scattering of the beam, leading to losses in beam energy and contents as well as creating an undesired background in the results due to gas atoms and molecules being brought along [Hellborg et al., 2005]. In graphitization, too, the quality of the vacuum is of the utmost importance, since carbonaceous particles from the air and from various components might otherwise be graphitized along with the samples, causingerrors in the final results. The quality of the vacuum-pumping equipment and the sealing, as well as the geometries of the system and the quality of the components themselves, play a vital role in the quality of the vacuum and thus in the accuracy of the end results.

Sources of gas

There are several reasons for the presence of gases in the system, relating to different components of the system. There will be gas in the system to begin with, for example, and so it is important to have good vacuum pumping. Leakages are another factor which may cause gas to enter the system, as the pressure is much lower on the inside of the system than on the outside. In this case, any system would benefit from having the opportunity to seal off various compartments of the setup, making it easier to check the system for leaks. Furthermore, there is a factor known as outgassing, which means that gases which were adsorbed, trapped or otherwise contained within the components themselves during manufacture or previous use are released into the vacuum, as explained by Danielson [2006]. Regardless of whether or not atoms of other gases are trapped in the components, however, the components themselves have a tendency to emit their own atoms, due to what is known as vapour pressure, when the pressure inside the system is low [Hellborg et al., 2005]. And finally, gas molecules may penetrate through the system components by adsorbing onto the outside of said components, diffusing through the material and being released into the vacuum inside. Through construction, choice of components and quality of the vacuum system, all these factors can be minimized, which is necessary for the accuracy of results, both in accelerator science and in ^{14}C measurements.

Materials with low rates of outgassing, such as stainless steel, aluminium, Pyrex and high density ceramics, are generally good starting points when choosing materials for vacuum components, as described by Danielson [2006]. Also, for each material, the other factors listed above must be considered, such as vapour pressure and permeation of gas molecules from outside the vacuum compartment through the materials of the compartment itself. The most commonly used materials are stainless steel alloys, along with aluminium alloys and other metals. Among the stainless steel alloys, the one called 304 SS is most common, as there exist other steel alloys which contain elements not suited for vacuum. 303 SS, for example, contains sulphur, which would ruin high vacuum.

Furthermore, the surface cleaning of the material chosen for the vacuum system is of importance. Organic contaminants must be removed, and there must be no porous surfaces caused by welding. The surface finish is also material-dependent, as for example anodized aluminium has the ability to adsorb much water vapour.

The O-rings and similar sealing components might also contribute to gas contamination of the vacuum system. If, for example, elastomer O-rings are used, these need to have been vacuum baked and not solvent-cleaned. Furthermore, it must also be considered that not all materials that fulfil the demands so far are optimal for each vacuum experiment. If other processes such as intense heat are involved, certain heat-sensitive materials would have to be ruled out, and a material would have to be chosen from those which are able to function well in high temperatures. Also, stainless steel components tend to undergo surface galling and become very difficult to disassemble from each otherunless they have been pre-treated to prevent such. If, on the other hand, electrical insulation is necessary, ceramics would clearly prevail over metallic alloys for those specific components. Sometimes, pre-treating or coating of various components is necessary, and it is important that what is used does not decrease the vacuum quality. An example is the use of molybdenum disulphide as lubricant between steel components. The dependence on process requirements is the final criterion for the choice of vacuum component material.

Flow parameters

Since gas pressure is directly related to the interaction of adjacent molecules, the interaction will be of a different sort when the pressure is very high compared to when it is very low. At normal atmospheric pressure and higher, the gas will behave much like a liquid in that there are abundant collisions between the gas molecules, meaning that they interact constantly, and the mean free path between collisions is very small [Hellborg et al., 2005]. The motion and flow of the gas becomes *viscous*. The viscous range is also divided into *laminar* and *turbulent* flow, based on whether the gas flows slowly or quickly [Hellborg et al., 2004].

The next general mode of motion is called *intermediary* flow, and sees the gas behaving partly in a viscous way and partly in a molecular way [Hellborg et al., 2005]. This regime is most prominent when the mean free path of the molecules is roughly equal to the dimensions of the evacuated system, which follows from the decreased gas pressure as some of the gas has been pumped out. This type of flow can be observed in the ion source of an accelerator as well as in the gas stripping compartment and in gas targets.

The final regime, closest to actual vacuum, is the *molecular* flow. The mean free path between collisions is now greater than the dimensions of the system, meaning that the molecules hardly ever interact with each other; the most common interaction is instead that of the molecules bouncing against the walls of the system.

The different regimes are not separated by sharp limits, but rather set as generally accepted definitions according to what is called the Knudsen number, *Kn*, defined as either $\frac{d}{\lambda}, \frac{\lambda}{d}, \frac{r}{\lambda}$ or $\frac{\lambda}{r}$ with the vacuum system diameter *d* and radius *r* using λ as the mean free path. With the first of these definitions, the limits for the three regimes are generally chosen so that viscous flow dominates when $\frac{d}{\lambda} = Kn > 100$, intermediary flow dominates for *Kn* between 100 and unity, and molecular flow dominates for *Kn* below the order of unity.

Next, it may be useful to define a set of parameters of the gas flow in order to better understand it. Looking at, for example, a pipe with different cross-section areas A_i, the gas will flow with different velocities v_i through said areas. The number of molecules per unit volume is set as n_i, giving a number of molecules passing the cross section per time unit of $N_i = A_i v_i n_i$. The volume which passes through a cross-section per time unit is given as $A_i v_i = S_i$, which is defined as the *pumping speed* according to Hellborg et al. [2005].

Having all N_i equal means that the difference in molecular density n_i between two adjacent regions will be proportional to *N*. The proportionality constant is called the *conductance* of the pipe, and it depends on the type of gas flow as well as the dimensions of the pipe itself. Conductances add the same way that capacitances do in electrostatics, i.e. in parallel connections as $C = \sum_{i=1}^{n} C_i$ and in serial connections as $\frac{1}{C} = \sum_{i=1}^{n} \frac{1}{C_i}$. The conductance of an aperture in the pressure range of molecular flow is given by Hellborg et al. [2005] as $C = A\left(\frac{RT}{2\pi M}\right)^{1/2}$, using *R* as the universal gas constant of $8.31\ J/(mol \cdot K)$, *M* as the molar mass of the gas remaining in the system (commonly air) and *T* as the absolute temperature. For a temperature of 293K (room temperature) and using the molar mass of air (0.029 kg/mol), this is proportional to the aperture area with a factor of 11.6. Listed by Hellborg et al. [2005] are also the conductances for two cases, that of a tube with a length-to-diameter ratio of more than 1.5 (long tube) and that of a tube with that same ratio being less than 1.5 (short tube). The former has the conductance $C = \frac{d^3}{3l}\left(\frac{\pi RT}{2M}\right)^{1/2}$ and the latter of $C = \frac{\frac{4}{3}d}{\frac{4}{3}d + l + \frac{d}{\frac{3d6}{l+7}}} A\left(\frac{RT}{2\pi M}\right)^{1/2} \approx \frac{d^3}{\frac{4}{3}d + l}\left(\frac{RT}{2\pi M}\right)^{1/2}$, both using *d* as the tube aperture diameter and *l* as the tube length. For an accelerator tube fitted with electrode apertures having the same aperture dimension as the tube itself, it is stated that the formula for a long tube is fully applicable.

Another convenient unit when dealing with vacuum is called *throughput* and is defined as $S_i p_i = Q$, where p_i is the pressure in point *i*. If there is no leakage into or out of the system, this value, which has the unit of power, is the same in all points *i* in the system.

Hellborg et al. explain in their article [2005] that the pressure gradient in a system with a constant contribution per enclosure surface unit to the outgassing, vapour pressure and gas permeation can be expressed as $\frac{dp}{dx} = \frac{q_d B}{CL}(L - x)$, where $\frac{dp}{dx}$ is said gradient, q_d signifies the contribution from outgassing, permeation and vapour pressure, *L* is the length of the system, *C* is the system conductance and *B* represents the circumference of the cross-sectional area of the system at that point *x*, which is the position between the pump, where $x = 0$, and the endpoint of the system, where $x = L$. Analytically, the pressure in the *x* direction can be found as $p_x = \int \frac{q_d B}{CL}(L - x)dx = q_D B\left(\frac{x}{C} - \frac{x^2}{2CL}\right) + constant$, where the constant is given by Hellborg et al. [2005] as $\frac{q_D BL}{S_p}$ with S_p as the pumping speed, meaning that the pressure in the *x* direction is $p_x = q_D B\left(\frac{x}{C} - \frac{x^2}{2CL} + \frac{L}{S_p}\right)$. It is also stated that the throughput through a length increment *dx* is $Q_x = C\frac{L}{dx}dp = q_D B(L - x)$.

Pump types

In this section, various types of vacuum pumps will be discussed, and the emphasis will be on those types of pumps which are employed in AMS at Lund University, either at Fysicum or at Geocentrum II. These pumps are one Pfeiffer Vacuum MVP 015-2 diaphragm pump which is used as roughing pump at the graphitization line at Geocentrum II, one Pfeiffer Vacuum TMH 071 turbomolecular drag pump used as high-vacuum pump on said setup, and one Pfeiffer Vacuum Duo 5 M rotary vane pump which supplies rough vacuum to the Fysicum graphitization line.

Rough and medium vacuum pumps

By the definitions of Oxford Vacuum Science Ltd. [2013], the regime of rough vacuum begins at atmospheric pressure and ends at 1 Pa, followed by the “process” vacuum range which reaches down to 10^{-2}Pa. As previously mentioned, there are no strict limits on these vacuum ranges, so the

definitions may vary between authors. Typically, pumps supplying “higher” than medium or process vacuumcannot operate at or near atmospheric pressure, which is why they tend to need “roughing” pumps in conjunction in order to be able to produce high vacuum.

Vane pumps

The rotary vane pump belongs to a subgroup of vacuum pumps called gas displacement pumps, as described by Pfeiffer Vacuum GmbH [2013 a, b]. These pumps operate by displacing gas from within the vacuum compartment towards either a later pump stage or directly out into the atmosphere. The rotary vane pump itself is oil-sealed, with a main design which is clarified in Fig. 3.

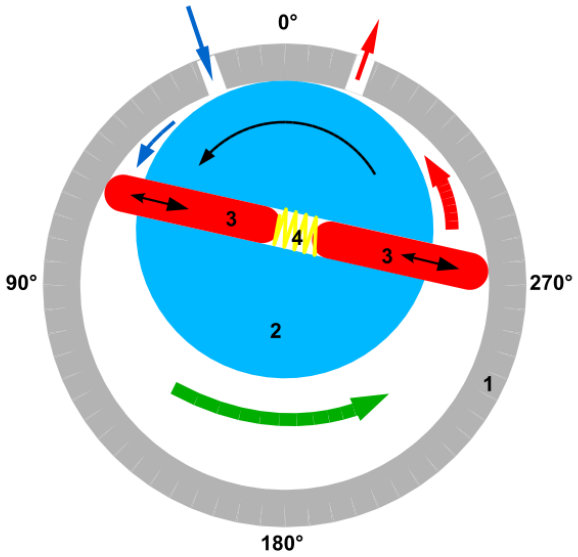

Figure 3: The general design of a rotary vane pump. 1: outer casing, pump body; 2: rotor, 3: vanes, 4: spring. Figure obtained from http://commons.wikimedia.org/wiki/File:Rotary_vane_pump.svg as of 2013-05-28. Creator: Rainer Bielefeld.

As the figure shows, the rotor is installed off-centre, and the vanes are flexible in the direction in which they extend from the rotor by means of springs. The outlet is sealed with oil, and the inlet is fitted with a vacuum safety valve. This valve is designed to close the connection between the pump volume and the volume to be evacuated if the pump stops. The gas inside the pump is used to vent the pump to stop oil from flowing back into the partly evacuated volume. As the rotor rotates, the vanes are extended and retracted by the varying distances between the rotor and the inner surface of the working chamber, and the two volumes change in size periodically. When the chamber opens to the inlet valve, the volume will be increasing, letting more gas in until the second vane passes the inlet and the gas is sealed off. The gas is then compressed as the volume gradually decreases again, building up pressure until the first vane passes the outlet. There, the gas is pushed out through the oil seal, and the vanes then let in the next quantity of gas from the inlet. The oil fills more than one function in the vane pump; not only does it seal the outlet so that no gas may leak back into the system, but it also lubricates the components, fills the gap between inlet and outlet so that no gas may return to the expanding volume, closes the gap between the vanes and the inner walls, and keeps the system at a suitable temperature by transferring away excess heat. Rotary vane pumps also come in two-stage models, which grant a lower final pressure.

Relevant remarks

The vacuum pump which is used in the graphitization system at Fysicum in Lund is of the rotary vane type, a Duo 5M two-stage pump from Pfeiffer Vacuum, as described by Pfeiffer Vacuum GmbH [2013c]. It is currently considered for replacement by another vane pump, mainly to remove the risk of oil getting into the graphitization reactors, as the current one relies on a cold trap with liquid nitrogen in order to prevent this. As implied in the heading, the rotary vane pump only supplies rough down to medium vacuum, meaning that further pumps are necessary in order to reach lower pressures. Rough vacuum pumps are typically used as auxiliary pumps or fore-vacuum pumps for those pumps that give better vacuum, such as the turbomolecular pump which cannot operate from standard atmospheric pressure but needs the pressure to be lowered first [Vacuubrand, 2013]. One of the weaknesses of the oil-sealed pump is that some oil particles may permeate into the evacuated volume, reducing the vacuum quality. There exist other models of rotary vane pumps which do not employ oil in the machinery [D.V.P., 2013 a, b, c]. D.V.P. describe the differences as that while oil-sealed pumps have lower final pressure, but only the oil-free can stand pumping at atmospheric pressure for prolonged times; the others need to be connected to sealed volumes whose pressures will decrease with the pumping. They also describe oil-lubricated pumps, being somewhat intermediary between the oil-sealed and oil-free types in their abilities and properties.

Diaphragm pumps

The diaphragm pump is a positive displacement pump, just like the rotary vane pump, with the significant difference that the rotary vane pump is oil-sealed [Danielson, 2006 b]. This means that the (rough) vacuum supplied by the diaphragm pump will be free from oil vapour. Diaphragm pumps are able to supply pressures down to approximately 1 Pa, and since they can operate under atmospheric pressure, they are quite suitable as rough vacuum pumps. The way these pumps work is by expanding, letting gas in, and then contracting to force gas out in another direction. In the first step, the diaphragm of the pump is pulled away from the pump to decrease the pressure inside the sealed volume. The inlet and outlet are equipped with one flapper valve each, the former only allowing air to enter and the other only allowing it to leave. As the pressure drops in the diaphragm volume, gas is let in through the inlet flapper valve, and as the diaphragm moves back again, the pressure increases, and the outlet flapper valve opens to let the gas out until the pressures are equal in the pump and in the outlet tube. So while each of the flapper valves opens as there is a net force in the one direction, it stays shut when the force direction is reversed, allowing for pumping to take place. The process is illustrated in Figs. 4 and 5.

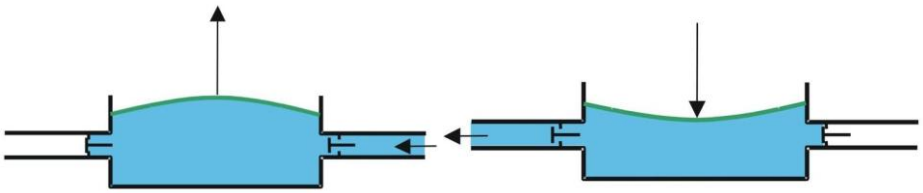

Figures 4 and 5. The design and operation of a diaphragm pump. The leftmost figure shows the pump with the membrane moving away from the pump, letting gas in. The rightmost figure shows the subsequent compression of the pump volume as the diaphragm moves back down, pushing the gas onwards through the outlet flapper valve. Figures obtained from *http://commons.wikimedia.org/wiki/File:Bomba_diafragma_aspirando.jpg* *and* *http://commons.wikimedia.org/wiki/File:Bomba_diafragma_impulsando.jpg*, *respectively, as of 2013-05-28. Creator: HUB.*

Relevant remarks

The setup at Geocentrum II uses a diaphragm pump, a Pfeiffer Vacuum MVP 015-2, as roughing pump, along with a turbomolecular pump for high vacuum. The latter pump type is described below.

High vacuum pumps

The range of high vacuum begins at 10^{-3} Pa according to Oxford Vacuum Science Ltd. [2013], and continues down to 10^{-7}Pa. As mentioned above, these pumps rely on being backed by roughing pumps.

Turbomolecular pumps

Molecular pumps in general, as described by Henning [1998], operate by transfer of momentum from rotating parts to the gas molecules. The velocity achieved by momentum transfer from the collision with the rotors is typically much larger than the thermal velocity of the gas molecules, and efficient pumping is possible when the mean free path of the molecules is greater than the distance between the rotating parts and the stationary components in the pump. This applies mainly for pressures below 10^{-1} Pa, in the molecular flow regime, where there is little interaction between molecules. For higher pressures, the interactions and collisions between the molecules prevents the pumping from being efficient, meaning that the molecular pumps cannot operate at or near atmospheric pressure, but need a rough vacuum pump to first bring the pressure down to the molecular flow range. The first molecular pump was introduced as a "molecular drag pump" already in 1913, but the general design was improved upon later on, in 1957, through the invention of the turbomolecular pump. The drag pumps had a relatively low pumping speed and were not entirely reliable, whereas the turbomolecular pump is considered reliable, consistent and capable of creating a very clean, high-quality vacuum. Henning[1998] describes it as the only mechanical pump which is able to reach pressures as low as 10^{-8} Pa (provided a rough vacuum pump has been used first). The pump consists of several sets of rotor-stator pairs, rotor blades tilted in one direction and stator blades in the other as seen in Fig. 6. The design is shown in the image below. The rotor blades spin very quickly, up to 500 m/s at the tips of the blades, and the pumping speed can reach several thousand litres per second.

Figure 6. A cut-through of a turbomolecular pump, showing the opposite inclinations of the rotor and stator blades. Figure obtained from http://commons.wikimedia.org/wiki/File:Cut_through_turbomolecular_pump.jpg *as of 2013-05-28. Creator: liquidat.*

Relevant remarks

The graphitization system at Geocentrum II in Lund employs a turbomolecular pump, a Pfeiffer Vacuum TMH 071, as a high-vacuum pump. Henning [1998] describes the turbomolecular pump as very popular in all fields that employ vacuum technology. As mentioned above, starting from atmospheric pressure, a turbomolecular pump needs a fore-vacuum or roughing pump, which in the case of the Geocentrum II setup is a diaphragm pump.

Diffusion pumps

Diffusion pumps depend on momentum transfer, and operate by heating a liquid until it vaporizes [Dayton, 1998]. The vapour is guided through a narrowing tube which quickly widens conically as the vapour is allowed into the vacuum chamber. The vapour forms a jet which expands and gains a high forward momentum, which is transferred to the molecules with which the jet collides. This pushes the gas out of the vacuum chamber, and the gas is subsequently led towards either further pumping components or out into the atmosphere. The vapour is condensed as the jet expands and cools down, and the fluid is led back towards the boiler to be used again. In order for the jet to be able to push the gas molecules along, it is important that there are not too many molecules in the way, which would lead to very many molecules gaining very little momentum. Therefore, the vacuum chamber needs to be pre-evacuated down to rough vacuum before the vapour jet technique is employed. This type of pump is called diffusion pump because the gas cannot diffuse against the flow of the vapour jet. The general design of such a pump is shown in Fig. 7.

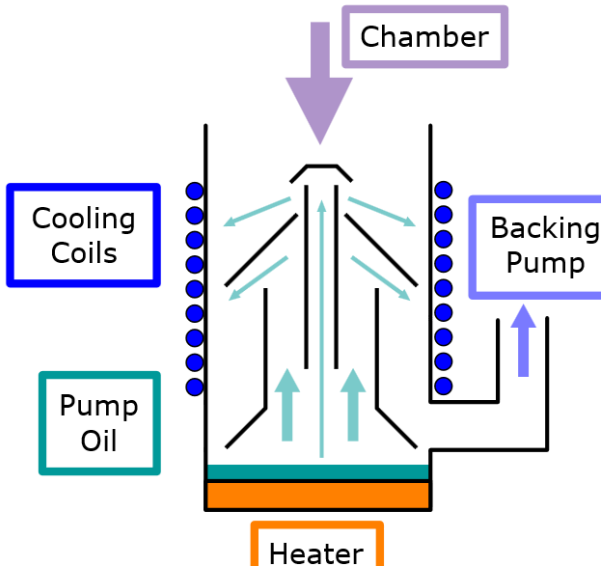

Figure 7. General design of a diffusion pump. As the liquid, in this case oil, is heated up and led up into the tubes which redirect it down, it forms a jet, pushing ambient gas molecules downwards. These are then more likely to be pumped out by the backing (roughing) pump. As the jet cools, the oil condenses on the sides of the pump housing and return to the heater. Figure obtained from http://commons.wikimedia.org/wiki/File:Diffusion_pump_schematic.svg as of 2013-05-28. Creator: Kkmurray.

Commonly, the liquid used is oil, which means that the use of such a pump in a graphitization line requires the use of a cold trap to prevent the oil from reaching the reactors. A previous version of the Fysicum graphitization line, however, relied on a diffusion pump using mercury. This was later removed, as the system of today uses only a rotary vane pump.

Cryopumps

Cryopumping is based on molecules losing kinetic energy when colliding with a cooled surface, and subsequently adsorbing onto said surface by means of dispersion and van der Waals forces, as discussed by de Rijke [1998]. The ability of a surface to adsorb molecules by these forces depends on factors such as chemical properties, the roughness or evenness of the surface, and the temperatures of the gas and the surface. The chemical properties determine, among other things, whether the dispersion forces between the gas molecules is strong enough to adsorb molecules, allowing for formation of many monolayers, or if the adsorption by dispersion forces happens only through the dispersion supplied by the surface molecules, allowing only a small number of monolayers at best. In general, cryopumping is a high vacuum technique, but it can also be used as a clean method of rough vacuum pumping, reaching pressures as low as 10^{-3} Pa.

Ultrahigh vacuum pumps

Using the definitions of Oxford Vacuum Science Ltd. [2013], ultrahigh vacuum requires a pressure below 10^{-7}Pa. There is no lower limit to this regime by this definition.

Titanium sublimation pumps

Working in a somewhat similar fashion to that of cryopumps in that they depend on adsorption, the titanium sublimation pumps and other similar designs using, e.g., barium rely on chemical adsorption ("chemisorption") rather than "cryosorption" [Ferrario, 1998]. Titanium is in this case evaporated or sublimed onto a surface, where it forms a layer with good chemisorption abilities, and while the same can be done also with some other metals, titanium is in general the most suitable for sublimation pumps.

Sputter ion pumps

The sputter ion pumps work to some extent thanks to the same principles as do the titanium sublimation pumps described above. They typically consist of cylinders of steel, acting as anodes, located between the cathode plates which are made of titanium, as explained by Schulz [1999]. There is a magnetic field along the axis of the anodes, and an electric field caused by the potential difference between anodes and cathodes. There are electrons being emitted from the cathode, which move in a helical fashion due to the magnetic field, which increases the likelihood that they collide with the gas molecules. When they do, typically a positive ion is formed, which is immediately attracted to either of the cathode plates. The ions then hit the cathode surface, knocking out (sputtering) titanium atoms and adsorbing onto the surface. The sputtered titanium atoms will eventually settle on some available surface.

Radioactive carbon dating with AMS

Sources of radiocarbon

The use of radioactive carbon for dating of organic material was first demonstrated by Willard Libby in 1952 [Currie, 2004], and would lead not only to a Nobel Prize in chemistry for Libby, but also to the development of what has become one of the most important dating techniques to date. Carbon exists in three naturally occurring isotopes, namely ^{12}C, ^{13}C and ^{14}C, of which only the latter is unstable, having a half-life of approximately 5730 years [NDT, 2010]. The relative abundances of the isotopes strongly favours the stable isotopes, with the atmospheric carbon contents being about 99% ^{12}C. Approximately 1% is ^{13}C, with the radioactive isotope making up only one part per trillion of the atmospheric carbon. ^{14}C is mainly produced through interactions between cosmic rays and the upper layers of the atmosphere, where the production of ^{14}C is a secondary process, as described by NDT [2013]. High-energy particles enter the upper atmosphere from space and interact with the atmospheric particles. Some of these interactions result in a neutron being knocked out of a nucleus. The neutron, having high energy, can then collide with one of the very abundant ^{14}N atoms, where it becomes part of the nucleus and knocks out a proton, resulting in the formation of ^{14}C. The carbon atoms formed this way tend to form compounds with the naturally abundant oxygen molecules, creating radioactive carbon dioxide, which is later absorbed by plants.

Thus it enters the food chain at the very first link, and since it has such a long half-life, it will be present in all higher life-forms, who feed on either plants, herbivores, or other carnivores. Since the quantity of ^{14}C is constantly replenished in all life-forms, the ratio between active and stable carbon remains in equilibrium with the ratio in the atmosphere for the duration of the individual's lifetime. At the time of death, however, plants stop absorbing carbon and animals stop consuming it, meaning that the ratio between stable carbon and active carbon will slowly change in a manner depending only upon the half-life of ^{14}C. This allows for a very precise age measurement technique which is based on counting the numbers of atoms of the different carbon isotopes. However, the ratio between stable carbon and ^{14}C in the atmosphere is not constant but tends to fluctuate somewhat [Damon, Lerman& Long, 1978]. This depends not only on the production of ^{14}C itself, which depends on the influx of cosmic rays and the extent to which these cause the production of ^{14}C, but also on human actions such as combusting fossil fuels and detonating nuclear bombs in the atmosphere. The former of these two factors decreases the relative concentration of ^{14}C as compared to ^{12}C, since the carbon stored in the fossil fuel consists of plant residues which have been dead for long enough to be nearly ^{14}C-free. The nuclear tests, on the other hand, caused an increase in the active carbon concentration to a far greater extent than the fossil fuel burning had decreased it. The effects of the bomb tests were mainly due to the fact that a nuclear explosion can be expected to release large amounts of neutrons which have their origin in the supercritical reaction that caused the explosion, and these are then able to interact with the atmospheric nitrogen, creating relatively vast quantities of radioactive carbon.

To complicate the situation further [NDT, 2010], certain plants are able to absorb less ^{14}C than they normally would given the atmospheric $^{14}C/^{12}C$ratio, depending both on plant species and local climate conditions, further complicating dating of humans and animals since it might not be known what plants were part of their diet, or in the case of carnivores, their diet's diet, nor what the climate situation was at that specific place at a specific time, seeing as the time is yet to be determined. The cosmic ray fluctuations themselves along with global climate effects have a rather large effect on the uncertainty of radiocarbon dating, as there is believed to have been a fluctuation in the concentration of ^{14}C of approximately 2% during what is called the Little Ice Age, taking place during the 16th to 19th centuries, as stated by Damon, Lerman and Long [1978]. This fluctuation is in the

same order of magnitude as that brought about by the burning of fossil fuels, both overshadowed by the increase brought about by the nuclear tests.

One way to deal with uncertainties regarding natural fluctuations and local climate effects is to test samples which correspond to precisely dated archaeological sites and times, in order to be able to calibrate the measured carbon ratios to find an approximate carbon ratio in the atmosphere at a given time in the past, as stated by NDT [2010]. Another method, as explained byDamon, Lerman and Long [1978], is called dendrochronology and is based on the fact that trees form new layers every year, following the cycle of the seasons, which can be seen as roughly concentric rings in the cross-section of the tree. The number of rings correspond to the number of years the tree has grown, thus offering a possibility to cross-reference any dating results with an actual value. However, there are a number of assumptions which must hold for this technique to be accurate: first and foremost, the ratio between ^{12}C and ^{14}C must accurately represent that of the atmosphere at all given times, thus assuming that the tree in question is not of the sort which are able to regulate their intake of ^{14}C; second, it must be possible to accurately determine the age of the tree from the tree rings, thus assuming that it has indeed formed one ring every year and that these are clearly visible to the naked eye or other detection equipment; and that the wood sample can be accurately analysed in order to determine its radiocarbon ratio. The latter depends on another crucial factor which must be compensated for: isotope fractionation. This effect means that certain processes favour specific isotopes over others, thus altering the ratios which would have been if there had been no fractionation. The process of photosynthesis has this effect, favouring the more abundant isotope, ^{12}C, over the isotopes with mass numbers 13 and 14, for the simple reason that the heavier isotopes react more slowly in the process of photosynthesis [Eriksson Stenström et al., 2011]. The discrimination is not constant, either; within a single tree, there may be variations of a few per mil, so a normalization must first be done.

Radiocarbon units and calculations

The normalization procedure introduces the quantity called $\delta^{13}C$, which describes the extent to which ^{13}C is fractionated in a certain process. This quantity expresses how much, in per mil, the ratio of $^{13}C/^{12}C$ has deviated from that same ratio of a specific standard material, Vienna Pee Dee Belemnite (VPDB). The lower this quantity is for a given sample, the more heavily is the ^{13}C isotope discriminated with respect to ^{12}C. Once the $\delta^{13}C$ is known, a fractionation factor is formed in order to translate the measured activity from, say, a sample of wood into the actual activity that it should have had if it had been wood with that specific fractionation of ^{13}C. Similar comparisons can be made also for ^{14}C. A more extensive treatment of this can be found in Eriksson Stenström et al. [2011].

The graphitization setup

Graphitization in Lund

Starting in 1987, the Pelletron accelerator was redesigned to be optimized for accelerator mass spectrometry, as described by Skog, Hellborg and Erlandsson [1992]. Since then, it has seen much use in the branch of ^{14}C AMS, which in turn has demanded that suitable samples of radiocarbon are manufactured for sputtering in the ion source, as previously outlined. Stenström [1995] lists a few possible ways to manufacture elemental carbon for sputtering out of organic samples, such as piston cylinder graphitization and cracking of carbon monoxide. The graphitization method which has been used at Fysicum and the GeoBioSphere centre, however, relies on the reduction of carbon dioxide catalysed by a metallic powder of the iron group. Since the method was developed by Vogel et al. in 1984, the procedure has seen some slight changes to further improve the process. Stenström [1995] describes two types of systems with some slight differences, one optimized for samples with a raised content of radiocarbon, higher than the content ratio of the atmosphere at the time, and another designed for lower ratios of $^{14}C/^{12}C$. The former is the setup at Fysicum, which has been updated a number of times. The latter line has been moved to Geocentrum II, and is described in Genberg et al. [2010] in its most recently updated form. The Fysicum setup is mainly used for modern samples (hence the high activity), also for applications other than dating. One of these is to check for occupational contamination of ^{14}C using hair samples, as described by Stenström et al. [2010]. Other uses for the high-activity line include microdosing studies; for further reference, see Stenström and Sydoff [2010]. The setup was recently updated (as part of this thesis) to be able to handle samples containing approximately 0.5 mg of carbon; before this update, it was designed for samples of a few milligrams of carbon [Stenström, 1995]. The low-activity graphitization system at Geocentrum II, on the other hand, is able to handle samples from 0.5 mg to 10 µg of carbon, and is applied mainly to graphitization of aerosol samples along with bomb pulse dating. Further explanation of the latter can be found in Hellborg and Skog [2008]. Sample preparation for dating of geological and archaeological samples is done using yet another graphitization system at the ^{14}C laboratory, also located at Geocentrum II.

Upgrade of the Fysicum graphitization setup spring 2013

In this section, the graphitization system at Fysicum is described in more detail, starting from the description by Stenström [1995] up to present day (spring 2013), including the upgrade which was performed as part of this thesis work.

Description of the system prior to upgrade

The pump used at the time Fig.8 was published (1995) was a mercury-based diffusion pump [Stenström, 1995]. This high-vacuum pump was deemedunnecessary, since the high-activity line does not require the same precision as the one preparing samples for dating.The mercury diffusion pump was thereforeremovedin favour of using onlyarotary vane pump. The influx of hydrogen gas was regulated by means of a needle valve, whereas a regulating valve was used for letting in fossil CO_2(containing only the stable carbon isotopes) in order to lessen the ^{14}C concentration in samples with too high activity, such as biological samples stemming from medical usage of ^{14}C. All the tubes were made of stainless steel with an outer diameter of 6 mm, which connected to other components and parts using Swagelok fittings, also made of stainless steel. The glass tubes which were to be heated were made of quartz glass, whereas the tubes used for cold traps are Pyrex glass. The dimensions were either 1/2” fitted with Cajon O-rings or 12 mm connected by means of Teflon ferrules in Swagelok fittings. The valves used were Nupro valves with the exceptions of one Hoke needle valve and one Hoke regulating valve, as seen in Fig. 8.

The production of carbon dioxide took place in its own subsystem of the main setup, which is located to the left of valve V1 in Figure 8. There were two types of glass tubes which could be attached to the leftmost end depending on what kind of sample was to be processed, both of which can be seen in the figure. The one which is attached in the figure was used for releasing CO_2 gas from carbonates, whereas the simpler straight glass tube seen below it was used for combustion of carbonaceous organic samples. These two could also be replaced with a cracker (seen below the two others in the figure), a flexible plastic tube used to crack open sealed quartz tubes. The CO_2 production volume was directly connected to a cold trap consisting of a Swagelok stainless steel tee with a 12 mm glass tube attached to it, and the pressure in the system could be measured using a Bourdon pressure meter. Between the valves V1 and V5 was the inlet volume, basically a section of steel piping connecting the production volume with the rest of the setup but with several pipes connecting to it in order to supply ^{14}C-free CO_2 and hydrogen, and to evacuate the system using the mercury diffusion pump. Past V5 was the measuring volume, in which the $^{14}CO_2$ gas could be added to the gaseous sample in order to dilute it. This dilution gas was added via the inlet volume, whereupon valve V5 was opened to let the two gases mix. The gases were moved from the one volume to the other by applying liquid nitrogen to the cold trap in the measuring volume. The pressure was measured using a Bourdon pressure gauge, which could be read off on a digital display.

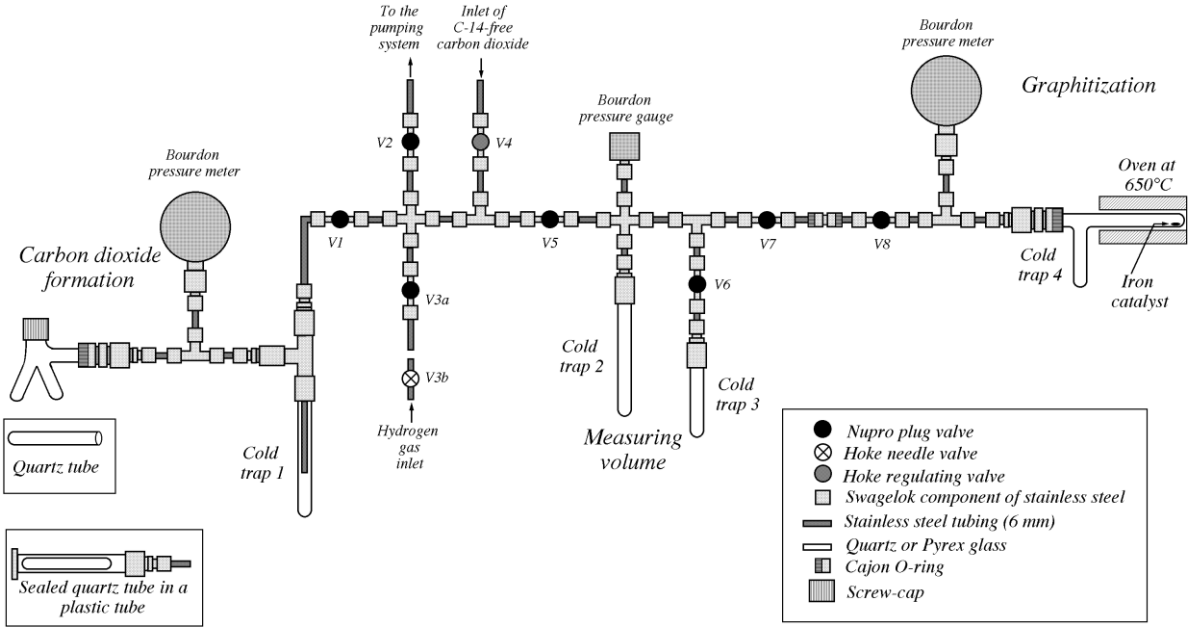

Figure 8. The graphitization line for high-activity samples at Fysicum, Lund University as of 1995. Used with permission.

To the right in the figure is the graphitization volume. The pressure was measured using the same kind of pressure meter as the gas formation volume, and the graphitization took place in a two-legged quartz tube consisting of a lower tube used as a cold trap and a reaction tube in which the carbon dioxide was eventually reduced into solid carbon, in a process which is described below. Placed around this part of the tube was a home-made oven at 650°C. The reason for the small section of piping between valves V7 and V8 was that the connection between the valves could be disconnected, meaning that the graphitization volume could be removed and replaced with another, allowing multiple samples to be graphitized at roughly the same time.

The low-activity system described abovediffered in several aspects. It used an oven near the middle of the system, containing silver wool and copper netting to capture halogen impurities in suspected

unclean samples. Several plug valves were replaced with Teflon-sealed glass valves, making them easier to take apart and clean between samples as this is necessary to a greater extent for samples with low activity. Another main difference was that the graphitization volume was vertical rather than horizontal, supposed to have better circulation which would shorten the reaction time.

In the time since 1995, there have been a number of changes to the Fysicum system as well. The mechanical frame has stayed roughly the same, but the mercury pump has been replaced with a rotary vane pump, there are now four stationary reactor volumes all connected to the setup and sealed off with their own shut-off valves, and the volume for $CO_2$is not currently in use. Combustion of samples currently takes place at Geocentrum instead, with the CO_2 samples being delivered to Fysicum in sealed quartz tubes, but future high-activity samples will be combusted at Fysicum. Furthermore, the third cold trap has been replaced with a cracker tube to crack the sealed tubes open near the measuring volume. The connections to the pump, the hydrogen supply and an argon supply are no longer to the left of the valve labelled V5 in Fig. 8, but rather connected between the measuring volume and the reactors. Thus, only those parts of the system which are to the right of V5 in Fig. 8 are currently in use, until on-line combustion will be re-implemented. There is no longer any inlet for CO_2; dilution of high-activity samples with fossil carbon is instead done before combustion. The Nupro plug valves have been replaced with shut-off valves, as implied above, whereas the needle valves remain. Several valves have new numbers or labels, as can be seen by comparing Figs. 8 and 9.

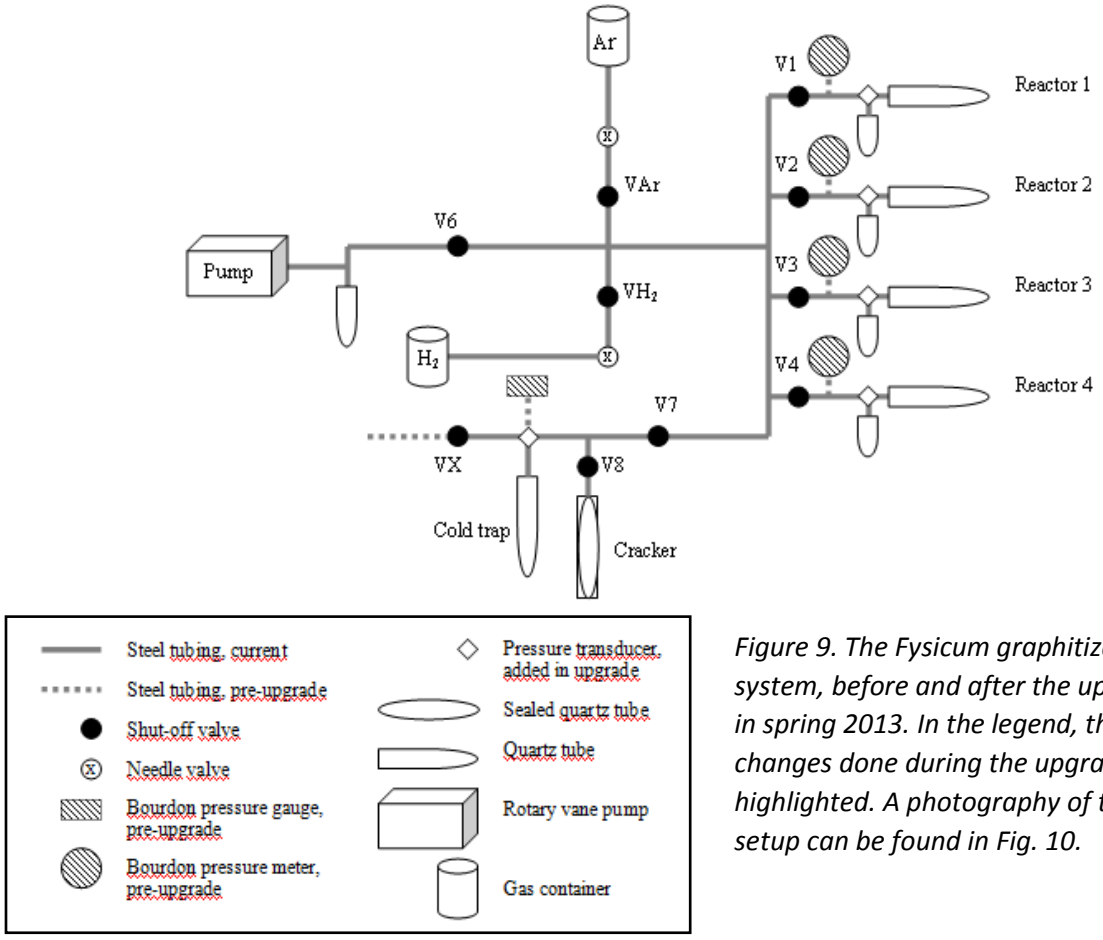

Figure 9. The Fysicum graphitization system, before and after the upgrade in spring 2013. In the legend, the changes done during the upgrade are highlighted. A photography of the setup can be found in Fig. 10.

Changes made in the upgrade

Much of the basic structure is unchanged, both the mechanical frame which supports the system and the piping of 6 mm outer diameter, as seen in Fig. 9. The main changes in the upgrade of spring 2013 involve the ovens, the reactor volumes and the pressure sensors. The reactor quartz tubes and the tees in which they are fitted have been switched out, replacing the former quartz tubes with new ones of outer diameter 3/8" and tees with openings of this size. The tubes for the cold trap part are of 40 mm length, and the tubes for the reduction reaction are 80 mm long. The tees are Swagelok stainless steel ultra-torr vacuum fittings (SS-6-UT-3). A hole has been drilled in each tee, allowing a pressure transducer (Fujikura XFGM-6 100KP GWSR) to be fitted in such a way that the pressure-sensitive end reaches inside the hollow inside of the tee. The transducers are glued into the holes using Huntsman Araldite 2000 PLUS in such a way that no glue has got inside the hollow part of the tee. All of the Bourdon pressure meters, including the one with a digital display, have been removed and replaced with tees fitted with pressure transducers. For this reason, the stainless steel cross above cold trap 2 in Fig. 8 has been replaced with a Swagelok tee (SS-6MO-3), with the pressure transducer in a drilled hole, just like the reactor tees.

The transducers are connected to aPico Technologies PP545terminal board via signal cables, whereupon the board transmits the signals from the transducers to a PicoLog 1216 data logger. Each transducer is equipped with two capacitors, one of 680 pF and one of 10 nF, which serve to reduce noise in the signal. The terminal board uses two types of resistors, 4.3 kΩ and 5.1 kΩ respectively, to reduce the voltage from the transducers to a level which the data logger can handle. The data logger receives the signals from the transducers, which can be read off on a computer using the bundled PicoLog software. The values are in the unit volt, and it is assumed that the voltage shown is linear with the pressure exerted on the transducers. The development of the pressure (voltage) over time can be monitored on a graph on the computer screen, and when graphitizing, it is helpful to be able to see the change in pressure over time.

New ovens, Watlow ceramic fiber heaters, replace the old ovens, and rather than being separate, the ovens are now mounted to the setup by means of four mounting rails, shown in Fig. 10. Two metal bars join each of the 3.3ft Swagelok mounting rails (303-S0-R-3.3) with the setup support frame. Mounted in each rail is a Swagelok support kit (304-S1-PP-10TM) held up by two rail nuts, also from Swagelok (SS-S0-RNM). Each support kit holds a 9 cm metal rod, to which is fixed a clamp holding an oven in place. All of the ovens are held up this way, allowing them to be slid on and off the reactor tubes. Each oven is connected to a variable transformer, with which the temperature of the oven is regulated. The four ovens use two different types of these transformers: two Tufvassons KIEA 8 and two Metrel HSN 0103 transformers.

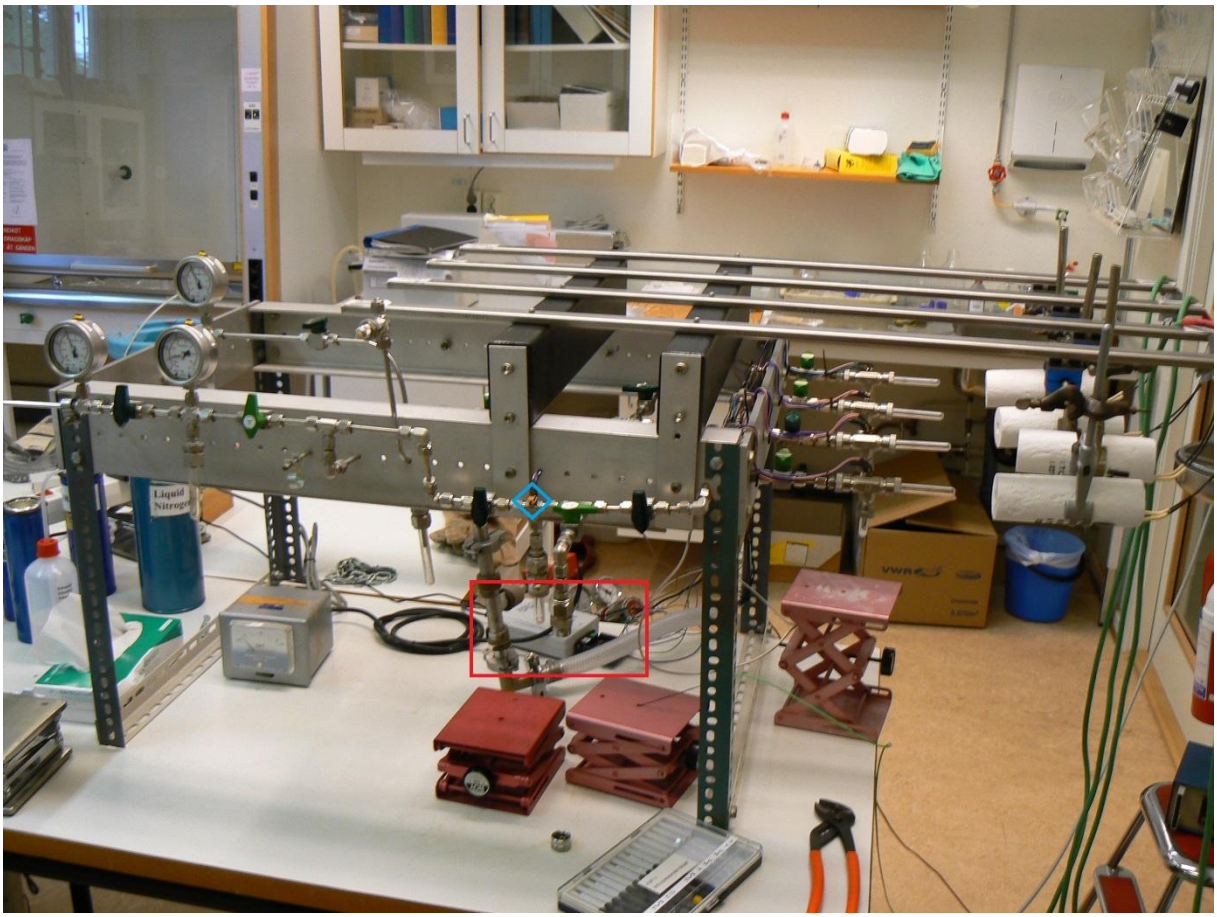

Figure 10. The graphitization system at Fysicum, post-upgrade. The rails supporting the ovens are clearly visible, as are the supports of the rails which were also added in the upgrade. The pump valve and the hydrogen inlet valve are obscured by the rail supports in this picture. The red rectangle highlights the PicoLog data logger with its terminal board, and the blue rhombus marks the location of one of the five pressure transducers.

Utilization of the Fysicum graphitization setup

In this section, the process of graphitization at the Fysicum high-activity setup is described, including preparation of some standard samples and the setup itself, and also the post-graphitization preparations necessary before the samples can be taken to the accelerator for analysis.

Preface to procedure

In this section, I will lay bare the different steps of the graphitization process as I have performed it. These graphitizations all serve the purpose of testing out the newly redesigned setup, and therefore are all different types of well-defined standards. Four different standards were tested out in each reactor to make sure that the system is operating as it should. The standards which were used were IAEA-C6 (sucrose), IAEA-C7 (oxalic acid), NBS-OxI and Acetanilide (from Merck pro analysi). The fact that two different oxalic acids are used (C7 and OxI) does not mean that one is redundant; the two have different activities and thus different isotope ratios. Further elaborations on these standards can be found in, e.g., Rozanski et al. [1992] and Le Clercq, Gröning and van der Plicht [1998]. The graphitized carbon samples were subsequently taken to the SSAMS facility at Geocentrum (described in Skog [2007] and Skog, Rundgren and Sköld [2010]), where they were isotopically separated as previously described. The sample preparation process is described below, along with the

graphitization itself as well as some necessary calculations regarding the different steps. The outcome from the accelerator runs are outlined and discussed in the Results section.

Preparation of samples

Throughout the entire process, carbon contamination of all components which will be in contact with the samples should be minimized, since any carbon which is added to the samples may alter the samples' carbon isotope ratios, thus rendering the samples useless for our purposes. For this reason, several steps are taken to clean the quartz glass tubes (7.5 mm inner diameter, 120 mm long, custom-made) which will contain the samples. First, the quartz tubes are baked in an oven, a Nabertherm L5/11/B170,for one hour at 950°C (i.e., 1223K), in order to remove residual carbon. Next, 800 mg of CuO is put into each tube, once it has cooled. The copper oxide will supply oxygen for the oxidation of the carbonaceous sample later on. Just like the tubes, the CuO had been pre-cleaned in an oven previously in order to remove any carbonaceous material. The tubes are then evacuated and filled with oxygen up to approximately half an atmosphere of pressure, and subsequently heated by an open LPG flame. This is to make sure that if there is any residual carbon inside the tubes, it will be oxidized into CO_2. The gases in the tubes are pumped out and the tubes are heated by the burner once again before they are ready for the samples. At this point, the samples are weighed up and placed inside the respective tubes, which have been marked on the outside with a permanent marker, an Edding 791 paint marker whose writing is able to stand very high temperatures.

It is important at this point to know what masses of the different sample types that correspond to which masses of elemental carbon. These values can be calculated, if the chemical properties of the sample substances are known. In the case of oxalic acid, which is hygroscopic [ChemicalBook, 2010], the value is instead taken from experience. The following masses are required to provide 0.5 mg of carbon:

Table 1. The masses required of the different standard samples in order to yield 0.5 mg of carbon.

Substance	Oxalic acid (OxI, C7)	Sucrose (C6)	Acetanilide
Chemical formula	$(COOH)_2$	$C_{12}H_{22}O_{11}$	$C_6H_5NH(COCH_3)$
Mass equivalent to 0.5 mg carbon	2.5 mg	1.2 mg	0.7 mg

When the samples are analysed in the mass spectrometer, the size of a sample is not of paramount importance, seeing as the spectrometer will provide chiefly the ratio between isotopes. The amount of carbon should be the same for all samples which are to be run in the accelerator at the same time, however, since the measurements show a slight isotope fractionation depending on the beam current, as described by Skog et al. [2010].

When the correct masses are known, the samples are weighed up using a high-precision weighing scale, a Sartorius 2004 MP, and placed inside the tubes along with a few milligrams of silver wire which has been baked in advance. The reason for this is that the silver will take care of sulphuric contaminations which would otherwise interfere with the graphitization process. The tubes are subsequently evacuated, whereupon they are sealed using a combined oxygen and hydrogen weld torch. The temperature becomes so high that even the quartz glass nearly melts, and the lower portion of the tube can be slowly pulled away, sealing itself as it is loosened from the upper part. The tubes are then placed in an oven, where they are heated up to 900°C (1173K) and kept at that temperature for 10 hours. It is during this part that the carbon in the samples is oxidized into CO_2,

and as they are taken out of the oven and cooled down by the surrounding air, they are ready for graphitization.

It is important, however, to make sure that the tubes will really be able to stand the pressure which they will be exposed to, as it is this point that yields the highest pressure upon the sealed tube. Since some of the tube's length is lost upon sealing, the length is no longer 120 mm. Approximating the length as 100 mm and with an inner diameter of 7.5 mm, the volume becomes roughly $4.4 \cdot 10^{-6}$ m^3. The temperature is known, which means that only the number of moles needs to be known before applying the ideal gas law. The target amount of carbon in the Fysicum graphitization setup is 0.5 mg, and since carbon weighs 12.011 grams per mole, this means that the system will be using 41.6 µmol of carbon. This is the amount of carbon dioxide which will be expected from the sample; however, here it will matter that carbon dioxide is not the only gas which will be formed within the tube. Due to the presence of hydrogen and the abundance of reduced oxygen, there will also be water vapour. CO_2 demands one mole of carbon from the sample whereas water needs two moles of hydrogen; this means that oxalic acid will add half as many moles of water as there is carbon, sucrose will add $11/12$ moles of water for each mole of carbon and acetanilide will bring $9/16$ moles of water per mole of carbon. Since the sucrose contains the most water, that will be used in the calculations. According to Dalton's law, $p = \sum_i p_i$, which means that the pressures of water and carbon dioxide are additive; this is reflected also in the fact that the ideal gas law is independent on what substances are involved as long as they have the same temperature and occupy the same volume. Thus, the number of moles of gas in total is at most 72.8 µmol. Inserting this into the ideal gas law, $p = \frac{nRT}{V}$, with R being the universal gas constant, gives a total pressure of approximately 161 kPa or 1.59 atm. The important question is whether the glass can take this pressure. According to ILPI [2013], using as wall thickness 1 mm (0.039 inches) and inner diameter 7.5 mm (0.295 inches), the maximal pressure that borosilicate glass of such dimensions can withstand is 275 psig, which equals a pressure of approximately 2 MPa. However, quartz glass is much more resistant to both temperature and pressure [Humi-Glas, 2013]. The calculationsapply for unharmed, perfectly preserved glass, whereas the sealed tubes have a weakness at the tip where they have been sealed. Here, the glass has a risk of being thinner, meaning that the pressure exerted upon this point might exceed what a sealed tube is able to withstand. However, since the pressure which they will be exposed to is more than ten times smaller than the maximum for borosilicate, which in turn is less pressure-resistant than the quartz glass used, even with the weakness it is unlikely that they would break under the pressure.

Graphitization

Preparations

The reactor quartz tubes containing iron powder and magnesium perchlorate (Merck $Mg(ClO_4)_2$), respectively, are prepared once their tubes have been cleaned and baked. The iron powder is essential, as it will act as catalyst for the reduction of the carbon dioxide with hydrogen gas. For 0.5 mg samples of carbon, 1 mg of iron is used. The magnesium perchlorate, which fills 4 mm of its tube, serves to absorb the water which is also formed in this reaction; further elaboration on the absorption of water by magnesium perchlorate can be found in Santos et al. [2004]. New perchlorate might have absorbed small quantities of water, so when the tubes are attached to the system, it is useful to evacuate the system, close the valves and leave it like that overnight. Once the perchlorate has been cleared of water in this way, it is good for use in a couple of graphitization reactions. When it needs changing, the grains will have developed a somewhat fuzzy surface. The powder is to be taken to the accelerator and sputtered once the carbon is reduced onto the iron, so using too much powder means that too many iron ions might get sputtered at the cost of the carbon ions which are wanted out of the sputtering. Using too small an amount, on the other hand, might mean that the

catalysis is insufficient for all of the carbon dioxide to be fully reduced, which means that the isotope ratios might be altered, either by random chance alone or also by isotope fractionation; furthermore, the iron is needed to conduct away heat from the carbon sample in the sputtering reaction, which means that there is such a thing as too little iron. Therefore, it is beneficial to try to keep the amount of iron powder as close as possible to 1.0 mg.

The graphitization process

At the earliest possible point before graphitizing, the ovens are be switched on and placed over the reactor tubes which contain the iron powder. This is to minimize the wait before the work can begin, since it takes the ovens roughly 20 minutes to reach the necessary temperature for the reduction reaction, which is around 600°C. The temperature is adjusted using the variable transformers, one for each oven. Two Dewar flasks containing liquid nitrogen and one containing ethanol are prepared, and liquid nitrogen is poured onto the ethanol in order to cool it down to a temperature between roughly -20°C (well below the freezing temperature of water) and -90°C (well above the freezing temperature of ethanol). All valves are closed, and the pump is switched on. One of the flasks containing liquid nitrogen is placed over the tube serving as cold trap for the pump while valve V6 is still closed, in order to freeze down and trap oil vapour escaping from the pump. This is done to prevent it from reaching any part of the setup where the carbon dioxide will be passing through, since the oil itself contains carbon which may have different isotope ratios than the samples. Furthermore, if any of the oil reaches the reactors, it can impede and even prevent the graphitization process. The pressure between the cold trap and the pump is monitored using an analogue pressure meter, and once the decreasing pressure has stabilized, valve V6 is opened along with valves V1 through V4 (leading to the reactors) and V7 (leading to the measuring volume). The cracker is loosened at the top, and the tube which will be cracked first is carefully inserted. Valve V8 (leading out to the cracker) is also opened. The computer and its pressure logging software are switched on, and a new measurement is started.

Valves V7 and V8 are subsequently closed, and the tube is cracked. The carbon dioxide is released into the cracker along with any residual gases which may have made it along with the sample so far. The most likely such gas is water vapour, and it is frozen down as the Dewar flask containing ethanol is placed over the glass tube at the lower end of the cracker. Since pressures tend to spread evenly over sealed volumes, and since at the one end the water vapour is steadily being frozen, the vapour will move towards the cold end until almost all of it has been frozen solid. This takes no more than a few seconds, and afterwards valve V8 is opened, letting the CO_2 into the measuring volume, over whose cold trap the remaining flask of liquid nitrogen is placed. By the process described above, this will now draw all the carbon dioxide in and freeze it down, since liquid nitrogen holds a temperature of -196°C or lower and CO_2, even at the low pressure inside the graphitization line, sublimes before reaching this temperature. As this process takes place, there will be a rather small peak in pressure in the measuring volume which results from the carbon dioxide passing as it moves from the cracker to the cold trap. Once the carbon dioxide is sublimed into a solid, valve V7 is opened, letting the pump remove any residual gases, whereupon valves V7 and V8 are closed again.

Now, the nitrogen flask is taken off the cold trap in order for the sublimed CO_2 gas to become gaseous again. To speed up this process, a cup of lukewarm water may be placed on the cold trap, or moved repeatedly on and off, so that the gas is released more quickly. The pressure will now rise in the measuring volume, and when it has stabilized indicating that all the gas is released again, the flask of liquid nitrogen is moved onto the magnesium perchlorate tube of the reactor which is to be used for this sample. It is good to be certain that the back end of the tube containing iron powder in that reactor is really at or near 600°C, since temperatures deviating from this by too far may lead to

other reactions taking place in the reactor than the desired reduction reaction. This might lead to formation of other end products, such as methane. Further descriptions of the chemical reactions involved can be found in Stenström [1995]. Once the flask is applied, valve V6 is closed along with the valves leading to the reactors which will not be used for this reaction, while the valve leading to the desired reactor volume stays open. Since the gas is about to be transferred to the reactor, it is useful to take note of the voltage read from the pressure transducer at vacuum pressure. This will be important when figuring out the amount of hydrogen that is necessary for the reduction reaction. Valve V7 is now opened, allowing the carbon dioxide to be transferred from the measuring volume into the reactor. The pressure in the former will drop to the vacuum level on the graph almost at once, but it is still wise to wait for a few seconds before closing the reactor valve. V6 is now opened, evacuating the measuring volume, and the cold trap is removed from the reactor. Once more the gas is to be thawed out, which may be facilitated with a cup of lukewarm water. The pressure in the reactor will now rise, and when it stabilizes, the pressure of the carbon dioxide can be read off. The absolute pressure of the carbon dioxide (in the unit volt as given by the pressure transducer) is found by subtracting the vacuum value from this value. Once this has been duly noted, the flask is applied again, sublimating the carbon dioxide in the magnesium perchlorate tube on the reactor volume, whereupon (after a few seconds, just to make sure) the reactor valve is opened to further ensure that there are no residual gases in the reactor. Valve V6 is subsequently closed, and the necessary amount of hydrogen gas is calculated.

The complete reduction requires two moles of H_2 per mole of CO_2, but since there will be very few molecules of CO_2 left near the end of the process, having a surplus of hydrogen gas is highly beneficial. Therefore, instead of letting in twice as much hydrogen as there is carbon dioxide, 2.4 times the CO_2 quantity is added. This proportionality between hydrogen and carbon dioxide quantities is exactly the same as the proportionality between their pressures, as given by the ideal gas law $pV = nRT$, since they occupy the same reactor volume at the same temperature.

The hydrogen is let into the system from its tube through valve H_2 until the pressure measured in the reactor reaches the appropriate level, whereupon valve H_2 is closed. If too much hydrogen has been let in, some can be removed by carefully opening valve V6 for a brief moment. When the appropriate amount of hydrogen gas is contained in the reactor, the reactor valve is closed. Now, the flask containing liquid nitrogen is removed from the lower reactor tube, releasing the carbon dioxide. In the presence of the iron catalyst, the reaction will begin almost at once, reducing the carbonaceous gas to solid carbon on the iron powder. On the pressure graph, this will be seen as a high peak as the CO_2 gas is released, reaching a highest value (which should be noted) and then starting to decrease. It will drop faster early on, taking on a more or less inverse exponential shape, so that at the end it will approach a constant value. When it does, the reaction has more or less stopped, although there are a few other parameters to consider. It is obvious that the more abundant the two gases are, the more likely to react are their molecules. Therefore, the sloping shape is the natural thing to expect. Typically, the reaction requires about four hours if the sample is as large as 0.5 mg carbon, as discussed in Stenström [1995], but the best way to determine when the reaction is completeis to look at how much the pressure has decreased from the highest value. Using the absolute pressures (measured voltage minus vacuum voltage), the decrease in pressure (voltage) from the maximal value reached is divided by the original absolute pressure of the carbon dioxide. If this quotient is equal to three, the reaction is complete, since the reaction uses up three moles of gas while producing only solid carbon and water which gets absorbed by the magnesium perchlorate. Of course, it is highly unlikely that every single molecule of CO_2 will have undergone the reduction reaction, given the statistical distribution of gases in a sealed volume and the fact that the reaction only takes place on the iron catalyst, but typically a value slightly less than three is enough to indicate

that a sufficient quantity of carbon has been reduced. If the ratio is significantly less than three, too little of the total quantity of carbon dioxide will have reacted, which means that there is a risk that isotope fractionation in the reduction reaction will have affected the results.

After the point where the reduction reaction has started and the peak value has been noted, the reaction will manage itself, and the next sealed tube can now be entered into the cracker. The valve V6 is opened along with the next reactor valve, the cracker is evacuated by means of opening valves V7 and V8, and once they are sufficiently evacuated (as indicated by the analogue pressure sensor), the valves V7 and V8 are closed again and the tube is cracked. This process is repeated until as many reactions are running as is desired (up to four at a time), and all that is needed is that one checks up on their pressure quotient (as mentioned above) now and then. When all reactions are considered complete, the system is ready for the next step.

At this point, the oven is taken off the reduction tube, and the reactor valves and valve V6 are opened, removing any residual gases from the reactor volumes. These stay open for approximately 15 minutes more, to increase the likelihood that residual and adsorbed gases are removed from the samples, whereupon the pump valve is closed again. Now, argon gas is let into the system from its tube via valve Ar. The argon gas is let in until it reaches roughly atmospheric pressure, as read out via the pressure transducers in either reactor. For reference on what order of magnitude this pressure is, the cracker can be removed from the setup, whereupon valve V8 is opened. Air will now enter that part of the system and reach the transducer in the measuring volume, showing clearly what voltage corresponds to atmospheric pressure. Keep in mind, however, that the transducers have different vacuum voltages, although all that is really needed is an approximate value. The argon gas is let in until its pressure reaches the desired level, whereupon the argon tube, the valve Ar and the reactor valves are closed. Tube caps of the proper dimensions (Swagelok 3/8” caps with Teflon ferrule, SS-600-C) are now prepared and labelled, whereupon the tubes are disconnected from the setup and the caps are put on. Since the air in the laboratory contains small amounts of carbon, it is good to be quick when putting the caps on. Argon is used in this step to keep the air from entering the tubes in this step, as would otherwise be the case, and being a noble gas, argon is a good choice since it will not react with the samples. In preparation for the next run of the system, it is helpful to at this point have prepared another set of tubes with iron powder and, if necessary, also a set of new tubes with magnesium perchlorate.

Pressing the samples

The samples now need to be pressed before they are ready to be taken to the accelerator. The pressing is done using a device from National Electrostatics Corp., the same company that also built the Lund SSAMS. The device is shown in Fig. 11. Throughout the procedure, cleanliness is vital, as there is a risk that the samples may become polluted with carbonaceous materials stemming from, for example, the experimenter’s hands and fingerprints, but also by each other since the equipment is the same for pressing all the samples. Therefore, ethanol is used frequently to clean the components used, and dust is removed by means of pressurized air. Everything is cleaned between samples, and no part which is to be used in contact with the carbon is handled by hand.

Figure 11. The sample pressing device, manufactured by National Electrostatics Corp.

The sample cylinder is placed inside the slot plate, upon which is placed a lid with a hole above the cylinder, so that there is a funnel leading the sample powder into the cylinder. Underneath the cylinder, there is a small peg which is screwed into the slot plate, to prevent the carbon from being poured through the hole in the cylinder and falling out underneath. The powder is poured from the argon-filled tube into the funnel, and a metal rod is used to knock on the side of the lid so that the carbon gathers as close to the hole as possible. The pressing machine is used to gently pre-press the powder into the cylinder below, only so much that the pressure sensor reacts. A small quantity of silver powder, less than one milligram, is then poured into the funnel on top of the sample, which serves to conduct away heat from the carbon sample during the sputtering, and after using the metal rod again to center the silver powder, the pressing machine is used to press the sample with a pressure of approximately 120 psi. The lid is now removed, the peg unscrewed and the cylinder picked up with a pair of tweezers. In order to make sure that there is no carbon or silver that is too loosely pressed, the cylinder is gently tapped against the slot plate. If nothing falls out, that cylinder is now ready for acceleration, and is therefore placed in a clearly labelled tube waiting to be taken to the accelerator. As before, the tubes are evacuated and filled with argon before the caps are put on. Along with the samples being prepared in this way are a number of “dummy” samples, which are not meant for analysis but rather for calibration of the accelerator (mainly the lenses and magnets) before the real samples are run. These are therefore placed first in the 40-slot wheel in which the other samples are put as well. The wheel is finally placed inside the ion source of the accelerator, and the samples are analysed.

Results and discussion

In this section, a brief calculation of certain flow parameters of the Fysicum system will be done. The results of the accelerator mass spectrometry of the standard samples will also be given and discussed.

Flow parameters

The Pfeiffer Vacuum Duo 5 M pump used for the graphitization line at Fysicum has a maximal pumping speed of 6 m^3/h and a maximal N_i of 30 s^{-1}. The inner diameter of the pipes is 2 mm, giving a cross-sectional area of about $1.3 \cdot 10^{-5}$ m^3. This area gives a maximal conductance of $1.45 \cdot 10^{-3} m^3/s$. As for the throughput, it varies with the pressure even at a constant pumping speed, but the highest pressure that is currently used in the Fysicum graphitization setup is atmospheric pressure, i.e. about 101.3 kPa, which yields a throughput of about 169 W. Assuming the system has no leaks, which has been found to be the case to a good approximation in the very most parts, this throughput will be the same in the entire system. The conductance will vary, however, as only the steel tubing is cylindrical and has 4 mm inner diameter; this is vastly different in, e.g., the reactor volumes.

AMS analysis

The following was interpreted out of the accelerator data (Table 2):

Table 2. The results of the accelerator measurements of the standard samples graphitized at Fysicum.

Type of sample	**Reactor**	**$\delta^{13}C$**	**pMC**	**σ(pMC)**	**$^{12}C^-$ (mA)**	**Remark**	**Final dp/p(CO_2)**	**Graphitization time**
Acetanilide	1	-25.9	18.69	0.17	16.4		2.347	7h 39min
Acetanilide	2	-19.4	15.55	0.15	17.5		2.993	7h 56min
Acetanilide	3	-31.9	3.02	0.07	17		2.386	8h 15min
Acetanilide	4	-28.4	21.35	0.21	12.9		2.810	7h 25min
C6	1	-12	148.42	0.65	13.7		2.844	7h 6min
C6	2	-15.9	149.91	0.73	21.1		2.949	7h 15min
C6	3	-22	148.92	0.78	8.4	Low ^{13}C	2.736	7h 43min
C6	3	-17.7	149.94	0.6	18.5	Retry	2.148	5h 1min
C6	4	-10.6	150.28	0.77	21.5		2.985	7h 53min
C7	2	-13.1	53.54	0.31	17		2.994	4h 8min
C7	3	-46.2	56.72	0.4	10.7	Low ^{13}C	1.097	4h 24min
C7	4	-12.3	51.02	0.47	13.4		3.000	4h 48min
OxI	-	-19	104.62	0.21	16.3		Approx. 3.	>7h
C7	3	-	-	-	0	No current; retry	1.032	6h 32min

The values obtained from the analyses of the OxI samples differ very little from one another, approximately two per mil. For this reason, the OxI samples were grouped together and used as a standard for the other samples. $^{12}C^-$ (mA) is the beam current of carbon-12 ions, and **σ**(pMC) stands for the uncertainty in the pMC (percent modern carbon) values. For further elaboration on the unit pMC, see e.g. Eriksson Stenström et al [2011]. The value of dp/pCO_2 shows how much the pressure has decreased from the peak pressure achieved when hydrogen and CO_2 begin to react, in units of how much CO_2 gas there was in the beginning, as discussed above. Final dp/pCO_2 means the value of

this quotient at the time when the graphitization was terminated, and the rightmost column of Table 2 shows how long the process had been given to reach that point.

In the appendix, the pressure graphs from the PicoLog data logger are listed as Figs. A1-A6. The blue, red, green and purple lines are the pressure curves of reactors 1-4, respectively, and the black line is the pressure in the measuring volume. The latter is of no consequence here, but when graphitizing it is very useful to be able to track the pressure in that volume as well. The vertical axis shows the voltage measured by the transducers, and the horizontal axis shows the time in seconds.

Two samples in Table 2 are marked “retry”. These samples felt necessary as the previous samples of those types in reactor 3 did not look right on the pressure graphs (see Figs. A2 and A3). Therefore, new samples of the same type were graphitized in reactor 3; these are the ones labelled “retry”. There are also two samples labelled “Low $\delta^{13}C$”, which means that the ratio of ^{13}C to ^{12}C is much lower than expected, indicating that the graphitization may have been incomplete. This is an indication that the graphitization was not complete, which can be suspected also from looking at the respective pressure graphs (Figs. A2 and A3). The correlation is clear, as the two samples which gave too small amounts of ^{13}C with respect to ^{12}C were the ones which prompted the “retries” of the respective sample types in reactor 3. One of the retries, however, gave hardly any current at all, which most likely indicates that that particular sample was lost in the pressing procedure. The same happened to the C7 sample from reactor 1, which is why it is absent from the table.

Starting with the acetanilide samples, they were rather far from the expected values. Containing only fossil carbon, acetanilide is expected to contain no ^{14}C whatsoever, which would correspond to its pMC (percent modern carbon) values being zero. This is not the case, as in Table 2 only reactor 3 comes close. The C6 samples showedslightly better proportions; the pMC values are mostly within the error margin of the expected value of 150.61, but the $\delta^{13}C$ values were off by a fair amount from -10.8‰, which is the expected value, except for the sample in reactor 4. The C7 samples were rather the opposite; whereas the $\delta^{13}C$ results were close to the expected -14.48‰, the pMC values fared worse with none of the samples within range of the expected value of 49.53. While in ^{14}C analysis the quantity of ^{13}C in a sample is not as interesting as that of ^{14}C, the $\delta^{13}C$ values still serve to indicate that not everything is as it should with the samples. However, the OxI results were close enough to the expected values that they could be used as a standard for the others, showing an unexpectedly small difference between the individual samples.

The most likely reason for the results described above is a leak in the cracker. Extensive leak detection has been performed on the entire system, but what has not been considered is that the cracker may let air in upon cracking a tube. The tests that have been performed have been so for long periods of no activity (up towards 65 hours), but no tests took into consideration whether the usage of the cracker was a cause for air getting into the system. A further indicator of the cracker starting to leak when a tube is cracked can be seen in Figs. A1 and A3, where the pressure begins to rise steadily after a while. For the time that the pressure rose, the cracker was letting air into the measuring volume. A way to detect this while graphitizing is that the freezing down of CO_2 in the measuring volume takes more than a few seconds. An example of what this looks like is given in Fig. 12, where the bump on the black curve around 5300 seconds shows the presumed presence of air having leaked in. If there were no leaks, the bump should hardly have been broader than the small peak just before 5000 seconds; instead, the gases present other than CO_2 were mostly not frozen down, but rather had to be pumped out, bringing an end to the bump on the graph. The presence of the air is also a likely reason for several graphitizations being somewhat incomplete (not having reached a $dp/p(CO_2)$ of or near three), as some of the air was presumably frozen along with the CO_2 and subsequently let into the reactor.

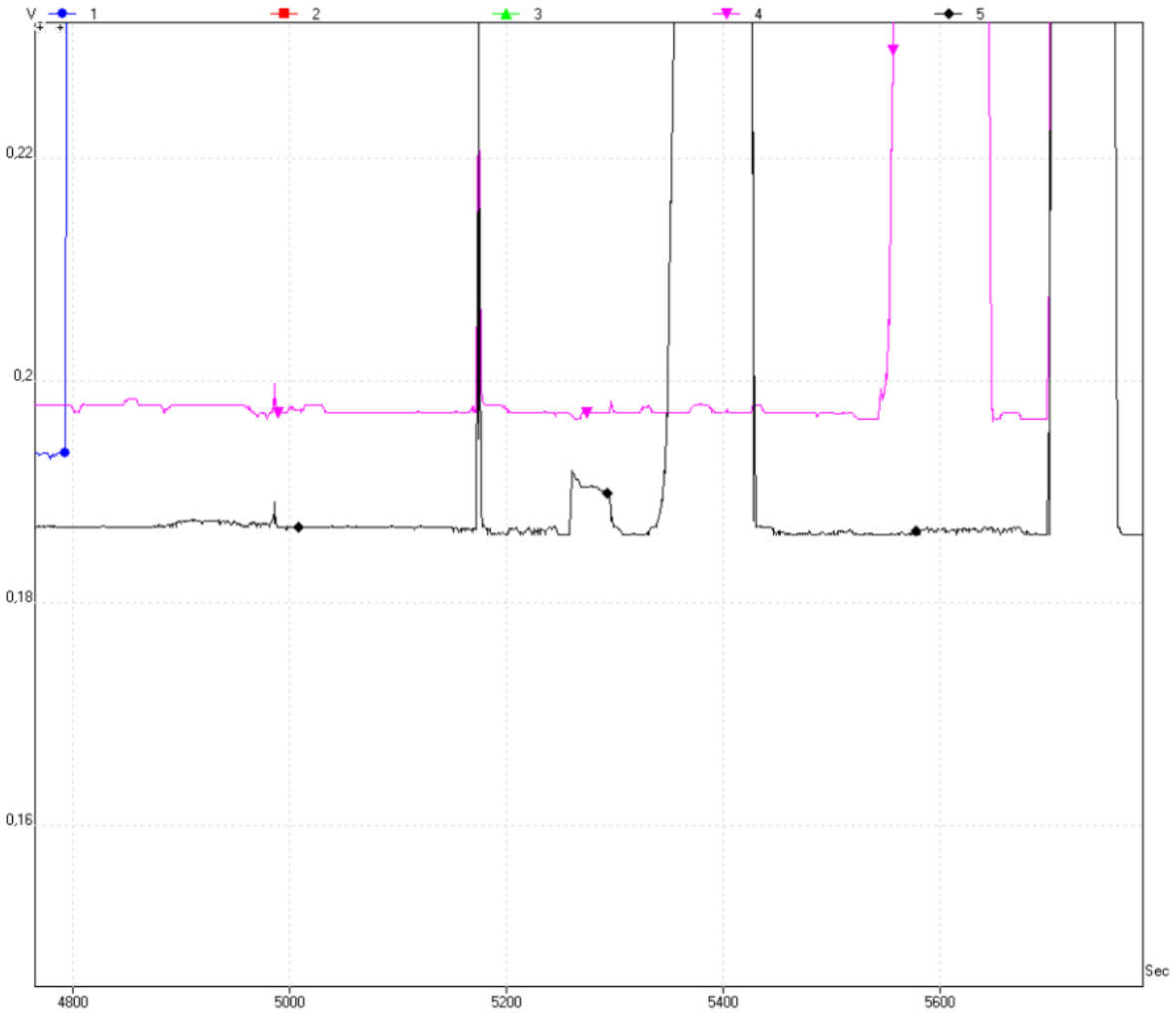

Figure 12. A part of graphitization graph seen in Fig. A4 in the appendix, zoomed in on the relevant region. Near 5300 seconds on the horizontal axis, the black curve shows a likely sign of there being air in the measuring volume when the carbon dioxide is transferred from the cracker to the measuring volume. The peak around 5000 seconds is a result of electronics noise, but shows roughly the expected width of the bump at 5300 seconds.

The atmosphere has its own ratio of the carbon isotopes, and when air leaks in, the ratios in the carbon dioxide are affected. OxI, however, is calibrated to have the same ratio as the contemporary atmosphere, which is why the OxI results were not only close to the expected value, but also unusually close together; it is reasonable to think that also the small differences between the samples resulted from air which had entered through the cracker. C7 has an activity which is significantly lower than the contemporary atmosphere, and it saw a raised pMC value; C6 has an activity which is higher than the atmosphere of today, and in those results, the amount of ^{14}C was lower than it should have been. These facts further support the hypothesis that the carbon dioxide had been diluted with air, affecting the isotope ratios of the samples.

However, the purpose of this thesis project has been fulfilled nonetheless; the graphitization system at Fysicum has been upgraded and modernized, tests have been performed and a likely cause for the detected errors has been outlined for future adjustment. The modernized parts of the setup have proven themselves to function as expected and passed the extensive leak detection. Furthermore, a

literature study has been performed regarding accelerator mass spectrometry, vacuum science and technology as well as radiocarbon dating, the results of which are found in this thesis.

Self-reflexion

As compared to other physics courses at Lund University, I have found this course (FYSK01) to be much more instructive in several ways. The responsibility placed upon the student is far greater than in most other courses, as there is little structure provided to the student other than what the starting point and final objective are. Furthermore, doing a thesis work allows the student to become much more immersed in the research field itself, which I found to be both more instructive and more motivating than merely attending lectures and performing a small number of experiments.

This thesis work has also offered me a much clearer viewpoint of what experimental physics is like. In the sessions of laboratory work during the first two years of physics education at Lund University, students would arrive at the lab, perform an experiment using equipment which is set up and more or less calibrated in advance. That shows very little what “real” experimental physics is like, which in my case has involved rather long periods of waiting for equipment to arrive and subsequently calibrating everything so that the planned experiments may be performed. Doing this thesis work has taught me that being an experimental physicist involves much patience and painstaking calibration, and I feel that I have learned some of this patience from my experiences during the course of this thesis project, which undoubtedly will come of use in the future.

Furthermore, this project has taught me much about accelerator mass spectrometry, vacuum technology, graphitization and experimental methods, and as mentioned above, getting the opportunity to perform this much experimental work has made me feel more acquainted with the course contents than most courses, if any, have. This kind of in-depth learning feels more rewarding, and will most likely live on in my memory for much longer than the contents of the lecture-based courses I have taken.

So to summarize my personal development gained from this thesis project, I feel that I have learned quite a lot, both with regards to physics, in experiment and theory, and with regards to the human virtue of patience.

Appendix

Here, the pressure graphs from the PicoLog data logger are listed. The blue, red, green and purple lines correspond to the pressures in reactors 1-4, respectively, and the black line is the pressure in the measuring volume. As previously explained, the pressures are given in the unit volt (V) which is the output unit of the pressure transducers; it is assumed that the voltage shown is linear in the detected pressure.

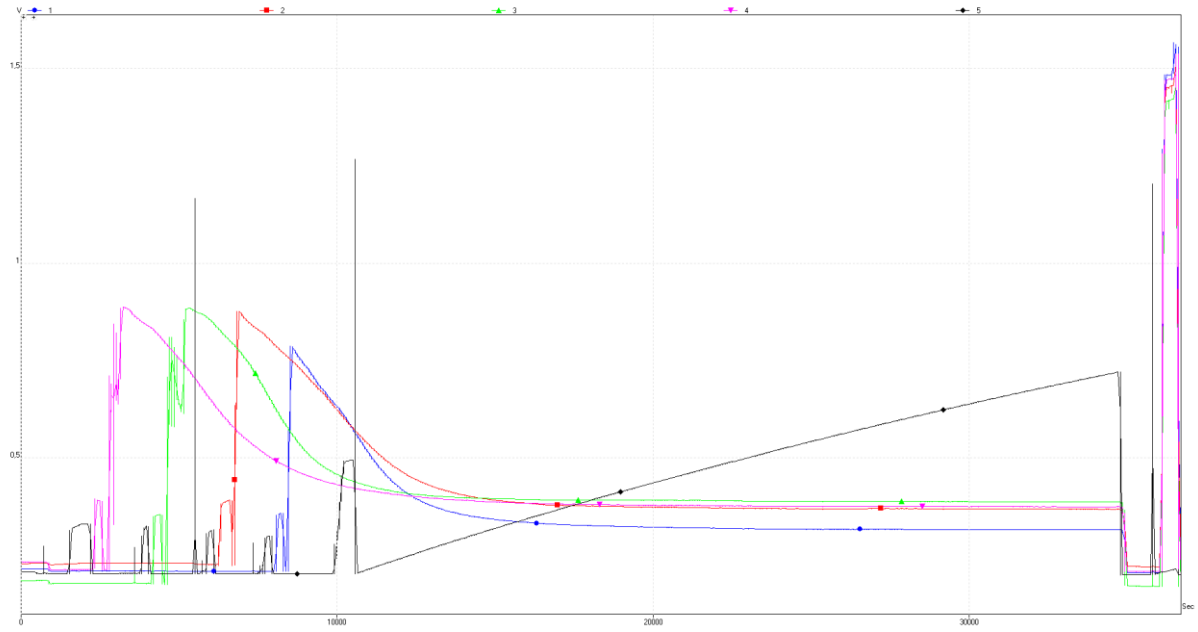

Figure A1. The pressure curves from the graphitization of the OxI samples. The rising pressure in the measuring volume most likely depends on the cracker continuously letting gas enter the volume.

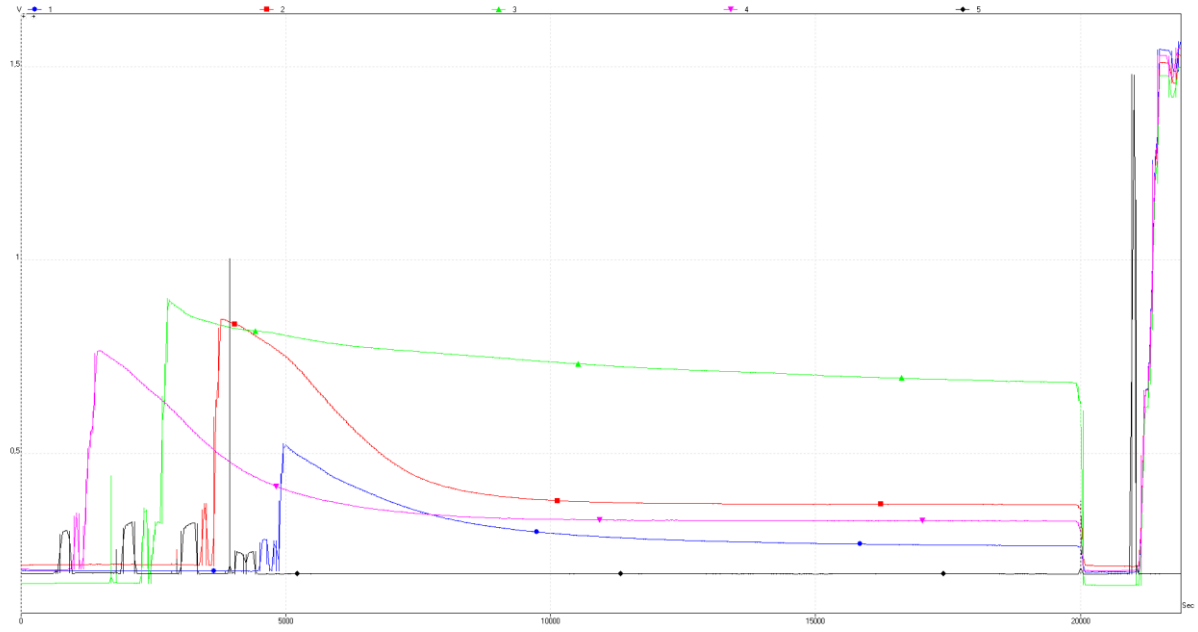

Figure A2. The pressure curves from the graphitization of the C7 samples.

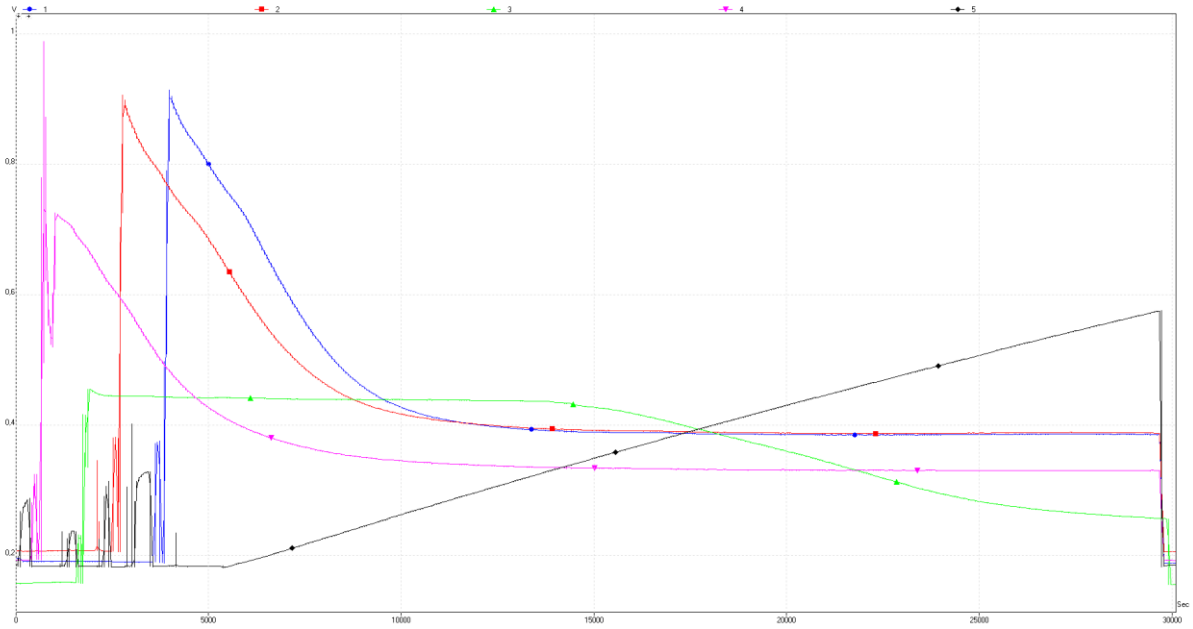

Figure A3. The pressure curves from the graphitization of the C6 samples. The rising pressure in the measuring volume most likely depends on the cracker continuously letting gas enter the volume.

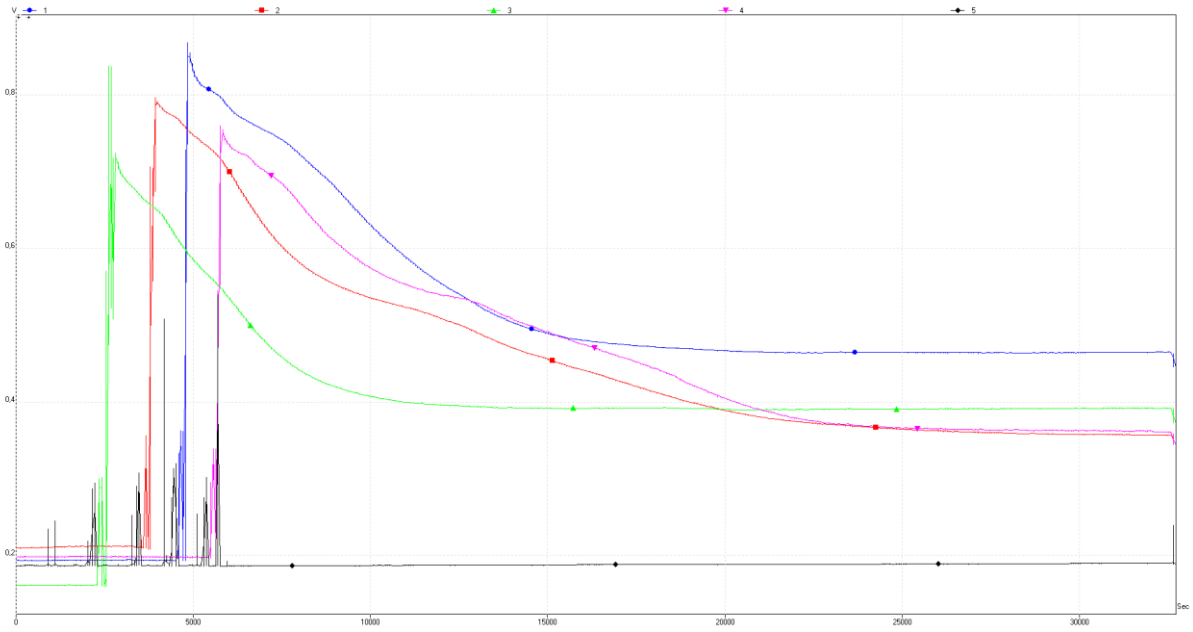

Figure A4. The pressure curves from the graphitization of the acetanilide samples.

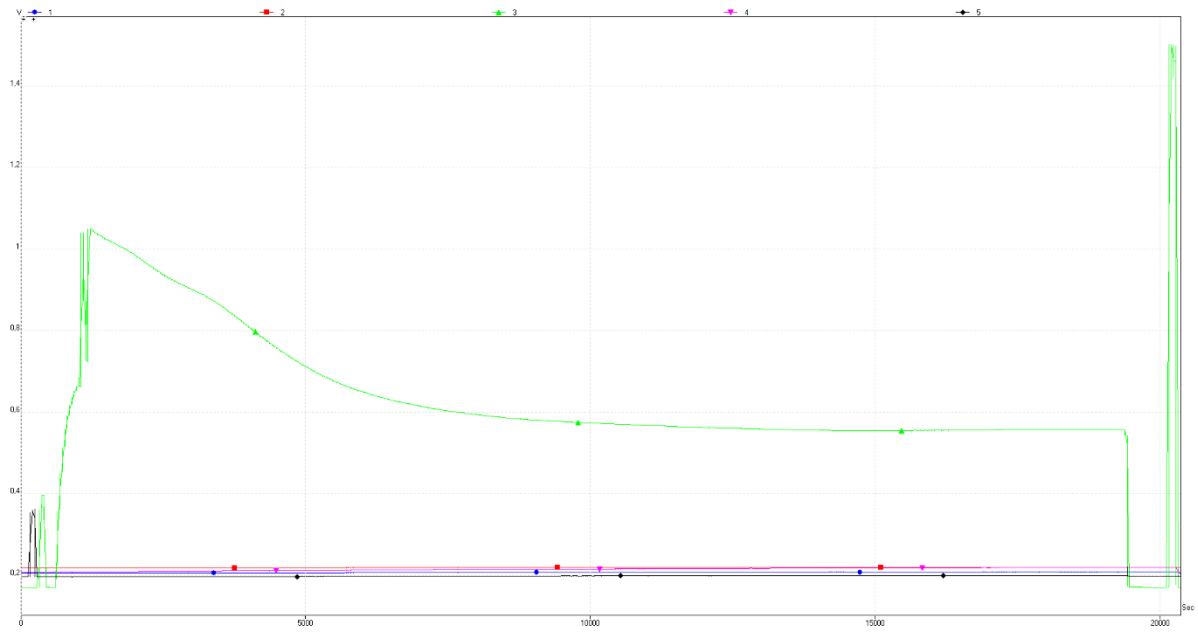

Figure A5. The pressure curve from a second graphitization of a C6 sample in reactor 3.

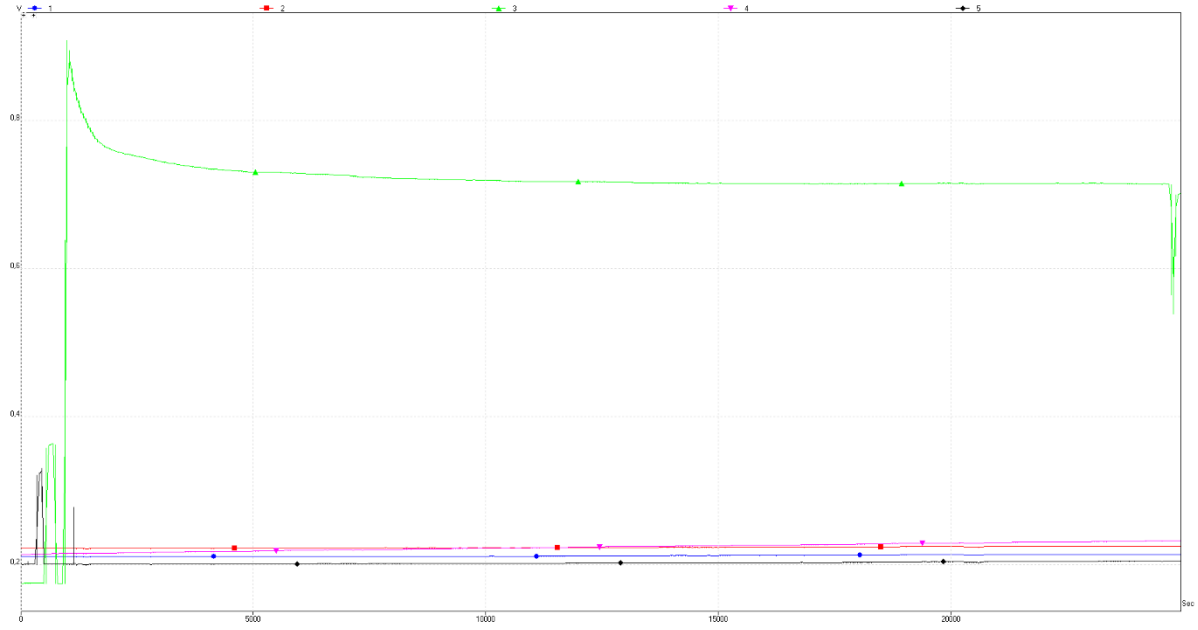

Figure A6. The pressure curve from a second graphitization of a C7 sample in reactor 3.

References

Alvarez, L.W., Cornog, R., *Helium and Hydrogen of Mass 3*, Phys. Rev. 56(1939), 379

Case Technology Inc., http://www.casetechnology.com/implanter/faraday.html, updated June 6, 1999, used as of2013-03-14

ChemicalBook, http://www.chemicalbook.com/ChemicalProductProperty_EN_CB0323998.htm, © 2010, used as of 2013-05-23

Currie, L. A., *The Remarkable Metrological History of Radiocarbon Dating [II],*J. Res. Natl. Inst. Stand. Technol. 109 (2004), 185-217

Damon, P. E., Lerman, J. C., Long, A., *Temporal fluctuations of atmospheric ^{14}C: Causal factors and implications*, Ann. Rev. Earth Planet. Sci. 6 (1978), 457-94

Danielson, P., *Choosing the right vacuum materials*, A journal of practical and useful vacuum technology #36, http://www.vacuumlab.com/articles.htm,updated2006-11-07, used as of 2013-05-30

Danielson, P., *How to choose a diaphragm pump*, A journal of practical and useful vacuum technology #17, http://www.vacuumlab.com/articles.htm, updated 2006-11-07 (b), used as of 2013-05-30

Dayton, B.,*Diffusion and Diffusion-Ejector Pumps,* in*Foundations of vacuum science and technology*, Lafferty, J. M. (ed.), Wiley-Interscience (1998)

deRijke, *Cryopumps*, in*Foundations of vacuum science and technology*, Lafferty, J. M. (ed.), Wiley-Interscience (1998)

D.V.P. Vacuum Technology s.p.a., http://www.dvppumps.com/vacuum_pumps_compressors.htm?v_lingua=ENG&v_categ_lista=00000-00007used as of 2013-04-10 (a)

D.V.P. Vacuum Technology s.p.a., http://www.dvppumps.com/oil_lubricated_vacuum_pumps.htm?v_lingua=ENG&v_categ_lista=00000-00005used as of 2013-04-10 (b)

D.V.P. Vacuum Technology s.p.a., http://www.dvppumps.com/oil_bath_vacuum_pumps.htm?v_lingua=ENG&v_categ_lista=00000-00006used as of 2013-04-10 (c)

Eriksson Stenström, K., Personal Communication (2013)

Eriksson Stenström et al, *A guide to radiocarbon units and measurements*, Internal Report LUNFD6(NFFR-3111)/1-17/(2011), Lund University, Dept. of Physics, Div. of Nuclear Physics (2011)

Ferrario, B., *Getters and Getter Pumps*, in*Foundations of vacuum science and technology*, Lafferty, J. M. (ed.), Wiley-Interscience (1998)

Fifield, L.K., *Accelerator mass spectrometry and its applications*, Rep. Prog. Phys. 62 (1999), 1223–1274

Genberg et al., *Development of Graphitization of µg-sized Samples at Lund University*, Radiocarbon, Vol. 52 (2010), No. 2-3, pgs. 1270-1276

Hellborg, R., Skog, G., *Accelerator Mass Spectrometry*, Mass Spectrometry Reviews 27(2008), 398-427

Hellborg et al., *Detailed calculations and measurements of the vacuum in an accelerator system*, Internal report LUNDFD6/(NFFR-3094)/1-16/(2004), Lund University, Dept. of Physics, Div. of Nuclear Physics (2004)

Hellborg et al., *Vacuum in an accelerator system – calculations and measurements*, Vacuum 78 (2005) 427-434

Henning, J., *Molecular Drag and Turbomolecular Pumps*, in*Foundations of vacuum science and technology*, Lafferty, J. M. (ed.), Wiley-Interscience (1998)

Humi-Glas, personal communication (2013)

Klody et al., *New results for single stage low energy carbon AMS*, Nucl. Inst. Meth. B 240 (2005), 463-467

Krane, K.S.,*Introductory Nuclear Physics*, John Wiley & Sons, Inc. (1988)

Kutschera, W.,*Accelerator Mass Spectrometry and Nuclear Physics*, Nucl. Inst. Meth. B 17 (1986), 377-384

Le Clercq, M., van der Plicht, J., Gröning, M., *New ^{14}C ReferenceMaterials with Activities of 15 and 50 pMC*, Radiocarbon Vol. 40 (1998), No. 1, 295-297

Litherland, A. E., *Accelerator Mass Spectrometry*, Nucl. Inst. Meth. B 5(1984), 100-108

NDT Resource Center, http://www.ndt-ed.org/EducationResources/CommunityCollege/Radiography/Physics/carbondating.htm, updated 2010-10-28, used as of 2013-04-22

NDT Resource Center, http://www.ndt-ed.org/EducationResources/HighSchool/Radiography/carbon14dating.htm, used as of 2013-04-22

Oxford Vacuum Science Ltd., http://www.oxford-vacuum.com/background/high_vacuum/regimes.htm used as of 2013-05-24

Patent Lens, http://www.patentlens.net/patentlens/patents.html?patnums=US_6815666&language=&#tab_0, used as of 2013-03-14

Pfeiffer Vacuum GmbH, http://www.pfeiffer-vacuum.com/know-how/vacuum-generation/pump-principles-and-vacuum-pump-performance-data/technology.action?chapter=tec2.1used as of 2013-04-10 (a)

Pfeiffer Vacuum GmbH, http://www.pfeiffer-vacuum.com/know-how/vacuum-generation/rotary-vane-vacuum-pumps/technology.action?chapter=tec2.2used as of 2013-04-10 (b)

Pfeiffer Vacuum GmbH, http://www.pfeiffer-vacuum.com/products/rotary-vane-pumps/two-stage/duoline/duo-5-m/onlinecatalog.action?detailPdoId=1904used as of 2013-04-10 (c)

Purcell, E.M., *The Focusing of Charged Particles by a Spherical Condenser*, Phys. Rev. 54 (1938), 818-826

Rozanski et al., *The IAEA ^{14}C Intercomparison Exercise 1990*, Radiocarbon Vol. 34 (1992), No. 3, 506-519

Santos et al., *Magnesium Perchlorate as an Alternative Water Trapin AMS Graphite Sample Preparation: A Reporton Sample Preparation at KCCAMS at the Universityof California, Irvine*, Radiocarbon, Vol 46 (2004), Nr 1, 165–173

Schulz, L., *Sputter-ion pumps*, CERN European Organization for Nuclear Research – Reports – CERN (1999)

Skog, G., Hellborg, R., Erlandsson, B., *AcceleratorMassSpectrometryat the Lund Pelletron Accelerator*, Radiocarbon, Vol. 34 (1992), No. 3, 468-472

Skog, G., Rundgren, M., Sköld, P., *Status of the Single Stage AMS machine at Lund University after 4 years of operation,* Nucl. Inst. Meth. B 26 (2010), 895–897

Skog, G., *The single stage AMS machine at Lund University: Status report,* Nuclear Instruments and Methods in Physics Research B 259(2007),1-6

Stenström, K., *New Applications of ^{14}C Measurements at the Lund AMS Facility,* Dept. of nuclear physics, Lund University (1995)

Stenström, K., Sydoff, M., *^{14}C sample preparation for AMS microdosing studies at Lund University with on-line combustion and septa-sealed vials*, Nucl. Inst. Meth. B 268 (2010) 924-926

Stenström et al., *The use of hair as an indicator of occupational 14C contamination*, Radiat. Environ. Biophys. 49 (2010,) 97-107

Vacuubrand GmbH + CO KG, http://www.vacuubrand.com/en-pageID1090.php used as of 2013-04-10

Walas, J. W. and ILPI, http://www.ilpi.com/glassblowing/glasspressures.html, used as of 2013-05-23

Wiebert et al., *The charge state distributions of 0.5-2.9 MeV Be, Al, Cl, Ti and Ni ions measured after carbon foil stripping*, Nucl. Inst. Meth. B 114 (1996), 15-19

Wittke, J. H., http://www4.nau.edu/microanalysis/Microprobe-SEM/Instrumentation.html, © 2008, used as of 2013-04-16